AN ABSTRACT OF THE THESIS OF

Peter Joseph Chace for the degree of Master of Science in Ocean, Earth, and Atmospheric Science presented on June 14, 2019

Title: INVESTIGATING ROTATING MICROELECTRODES FOR RAPID IN SITU DETECTION OF DISSOLVED OXYGEN

Abstract approved: _____
Clare Elizabeth Reimers

Rotating disc electrodes (RDEs) exploit the induced flushing of a radially spun electrode to increase the overall rate of analyte flux to an electrode sensing surface and its resulting signal current (*i*). Here initial efforts to evaluate a rotating platinum (Pt) microelectrode for efficacy as a rapid in situ dissolved oxygen (DO) sensor when submerged in natural waters, particularly seawater, are reported. The sensor tested employs a polished Pt disc (r = 50 µm) working electrode fixed at the tip of a rotating shaft as part of a three electrode system that includes a large surface area Pt wire (r = 250 µm) as a counter electrode and a silver/silver chloride (Ag/AgCl) reference electrode. An applied voltage (E = -0.75V) set between the Pt working and the reference leads to the reduction of molecular O_2 at the disc surface and flow of electrons from the counter to the working electrode. This resulting electrical current was verified to be linearly proportional to concentrations of dissolved oxygen from 30 – 330 µM in seawater (S = 34), with sensitivities of ~0.6 nA / µM at 1000 rpm, when the electrode was run in a

chronoamperometric mode. A similar linear range was also found in filtered fresh water collected from rivers. Evidence from flume experiments revealed shorten response times ($t_{90\%} \leq 0.10$ s) compared to the majority of commercially available sensors, the result of both the rotational flushing of the electrode surface and the use of a bare Pt surface with no membrane.

Physically durable, and an order of magnitude faster in response than the majority of reported aqueous DO sensors ($t_{90\%} > 1.0$ s), further optimized RDE systems similar to those detailed here could be used to resolve DO at high frequencies (2 - 18 Hz) in either fixed-point Eulerian or fast water column profiling applications. This first reporting of a truly in situ watertight electrode rotator additionally demonstrates the practicality of translating other RDE techniques to in situ detection.

INVESTIGATING ROTATING MICROELECTRODES FOR RAPID IN SITU DETECTION OF DISSOLVED OXYGEN

By
Peter Joseph Chace

A THESIS

Submitted to

Oregon State University

in partial fulfillment of
the requirements for the
degree of

Master of Science

Presented June 14, 2019
Commencement June, 2020

Master of Science thesis of Peter Joseph Chace presented on June 14, 2019.

APPROVED:

_____
Major Professor, representing Ocean, Earth and Atmospheric Science

_____
Dean of the College of Earth, Ocean and Atmospheric Science

_____
Dean of the Graduate School

I understand that my thesis will become part of the permanent collection of Oregon State University libraries. My signature below authorizes release of my thesis to any reader upon request.

_____
Peter Joseph Chace, Author

ACKNOWLEDGEMENTS

First I would like to thank my advisor, Dr. Clare Reimers, for all her support and guidance starting from my time as an undergraduate intern in her lab. Since then Clare has been an immovable source of knowledge and sound advice, and I have her to thank both for the start of my career and for leaving me with an example I will always look back to of what it takes to be a responsible and productive scientist. I would also like to thank my committee members, Drs. Burke Hales, Jonathan Fram and grad rep Julie Tucker for their help in bringing this project to completion.

I must also thank the many people whose technical expertise, advice, edits, and labor helped to make this work possible, as I certainly did not do it all alone. These include but are by no means limited to Yvan Alleau, Miranda Bradley, Jeremy Childress, Kent Fletch, Jay Simpson, Ben Russell, Adrienne Chan, Cheng Li, Kristen Fogaren, Lori Hartline and of course Donald Nuzzio who built and serviced the potentiostats. It is here I must again express thanks to Dr. Reimers for originating the in situ concept that began this particular line of investigation.

Lastly I'd like to thank my family: Christopher, Daniel, and Deborah, who continue to be an unflinching source of support, affection and grounding, absent of which I would not be here.

TABLE OF CONTENTS

LIST OF FIGURES

The following work is dedicated to Joe and Dolores. Who both told me to run as fast as I could toward the things I cared about, and wouldn't understand a word of this.

1.0 Introduction

1.1 Resolving dissolved oxygen

Dissolved molecular O_2 (DO, or bulk aqueous phase [O_2]) is a key biogeochemical parameter in marine and limnologic settings. Changes in DO reflect biotic and abiotic transformations within water masses and the various transport mechanisms that drive solute exchange across system boundaries. The primary oxidant of marine organic material and one of the most reactive seawater constituents, this essential ocean variable (Lindstrom et al. 2012) is routinely used to trace biological production and metabolism throughout the ocean. As investigations of ocean biogeochemistry shift more to in situ methods and call for accurate measurement at finer and finer spatial and temporal scales, there is an impetus to explore different sensing approaches that could push the limits of response time, signal stability and physical durability for functional DO sensors.

While DO sensors have progressed significantly since their early inceptions (Clark 1953, 1956, Carritt and Kanwisher 1959), modern devices built to function submerged in seawater are not free of limitations and assumptions. Commonly cited issues that can become problematic in different applications include poor physical durability, limited response times, and a difficulty to maintain long term signal stability due to biological fouling of sensor surfaces (Delaney et al. 2010,

Denault et al. 2009). In the majority of settings the capabilities of the most common DO probes are adequate. However, a limited number of in situ measurement techniques being applied in fast flowing waters have been found to require capabilities of response time and durability beyond that afforded by most or any commercially available sensors. It was improving the hardware for one such approach, Aquatic Eddy Covariance (AEC), that prompted this study of an alternative DO sensor based on a rotating microelectrode that could in theory respond at rates faster than current sensor formats allow.

A specialized in situ approach used to determine DO fluxes across the sediment-water interface, AEC comes with a demanding set of sensor criteria (Berg et al. 2003, Falter et al. 2008, Lorrai et al. 2010, Holtappels et al. 2013, Donis et al. 2015). The AEC method requires the accurate resolution of DO in a small (<5 cm^3) fixed control volume at time scales that can capture DO fluctuations caused by natural turbulent eddies that move bottom waters to and away from the benthic interface. In aquatic environments with low turbulence such as deep lakes and marine basins, the typical $t_{90\%}$ of ~1 s ($t_{90\%}$ being the time it takes for 90% of a sensor's signal to respond to a change in bulk concentration, or the functional response time) of most fine-point commercial sensors is appropriate. When in higher energy settings, however, smaller eddies can operate at time scales as short as 0.2 s (Lorrai et al. 2010). The fastest available sensors ($t_{90\%}$ ~0.5 s, Berg et

a. 2016, Merikhi et al. 2018) are unable to meet this lower threshold, and thus it is possible in some instances a significant portion of mass flux may be missed (Reimers personal communication), underestimating eventual DO flux determinations..

Another challenging criterion for AEC is the need for DO measurements to align in time with the velocity record. While this can be helped by physically positioning the sensor at the edge of the velocity measurement volume, the measurement volume and oxygen probe cannot actually overlap (as this corrupts the velocity measurement). Thus, there is always some small spatially induced, flow direction-dependent, time difference that must be corrected for. In addition to this spatial offset, the response time of the sensor must also be accounted for when correlating time series. During alignment of the records, small 0.2 s shifts in one direction or another can in the worst scenarios create a bias that doubles or halves the eventual calculated flux (Berg et al. 2015). While there will always be a need to correct for the spatial offset between the DO and velocity measurements, reducing sensor response time as much as possible will greatly reduce error and uncertainty.

Recent work has also shown inconsistencies in the response time of individual microoptode sensors of common manufacture ($0.15 < t_{90\%} < 0.59$ s, $n = 10$) used

regularly in AEC (Merikhi et al. 2018). This ~0.44 s range speaks to the difficulty of applying a fixed time shift to resulting AEC records from multiple deployments. While different *post hoc* mathematical treatments have been developed for unidirectional flow and under-wave scenarios, there is no perfectly settled procedure that can determine an ideal time shift universally under all conditions. DO sensors able to respond on a millisecond timescale would eliminate the uncertainty from the sensor's response lag and produce much more readily aligned records of DO and velocity variations. This benefit would also be applicable to existing CTD and mobile sensor platform configurations where reduced DO sensor response times could also eliminate the need to apply response time corrections and greatly improve the overall resolution of water column profiling (Daly et al. 2004). While the motivating goals of this investigation were an improved sensor for AEC, there is clear potential for further developed rotating electrode systems to be a powerful tool for water column profiling.

1.2 Background on aqueous oxygen sensors

1.2.1 Electrochemical sensors

The first sensors used for determinations of DO in aquatic environments were electrochemical and adapted from Clark (1956) (Carritt and Kanwisher 1959, Reimers et al. 1986, Oldham 1994, Gieseke and de Beers 2008, Berg et al. 2009, McGinnis et al. 2014). 'Clark-type' or 'polarographic' macro and microelectrodes today still employ the reduction of O_2 on Pt or Au after diffusion of O_2 through a membrane, although progressive refinements have reduced fouling, lowered limits of detection (Revsbech 1989), improved signal stability (Revsbech and Ward 1983), and proliferated a multitude of morphologies (Oldham 1994, Suzuki et al. 2001, Lee et al. 2008). Similar gains have been made with in situ galvanic-type microelectrodes (Curtin et al. 2005, Crimmins et al. 2005, Johnson et al. 2011, Else et al. 2015), which while fairly stable consume their internal reactants and have a limited lifespan of months to years (Nei and Compton 1996). The vast majority of these microelectrodes are also constructed within thin glass outer capillaries that make them inherently fragile. The ease of breakage from animal strikes in situ, or user error during handling, increase costs and can limit the usable data produced during deployments. Approaches to cover and protect sensors (e.g. in flow through cells, with caps or guards) can reduce this damage, but also introduce artifacts and retard direct communication with the surrounding environment.

Electrochemical approaches inherently utilize the direct consumption of molecular O_2 and in doing can generate highly reproducible sensor responses that are linear with respect to oxygen concentration with definable temperature and ionic strength effects (Brendel and Luther 1995, Pletcher and Sotiropoulos 1996, Gundersen et al. 1998; Sosna et al. 2007, Hutton et al. 2008). This linearity simplifies calibrations allowing defined equations for signal current (i) at particular formats of electrode. Most of these equations are underpinned by or stem from early definitions of electrode current responses in benchtop steady state conditions.

An example, eq 1, defines the steady-state current at an immobile disk electrode, as in diffusion-controlled chronoamperometry.

$$i_{ss} = 4nFD_O C_O^* r_0 \qquad (1)$$

Another, the Cottrell equation (eq 2), defines current response over time to a stepped shift in potential at the same disc.

$$i(t) = \frac{nFAD_O^{1/2} C_O^*}{\pi^{1/2} t^{1/2}} \qquad (2)$$

Wherein n is the number of electrons involved in a given reaction, F is Faraday's constant, r the radius of the electrode, C^*_o the concentration of the electrochemically active analyte in bulk solution, A the area of electroactive surface, and D_o the molecular diffusion coefficient of that analyte. Both of these

non-rotating analogs of the hydrodynamic system detailed later in this study, seek to define behavior at a planar electrode with no membrane in steady state benchtop conditions usually assumed to be at standard temperature and pressure (298.15 K, 1 atm). More familiar commercial Clark-type sensors are built on these fundamental electrode concepts, but additionally must consider the influence of membranes and internal electrolyte and junction effects. As such, the signals produced by many sensors with membranes are only loosely definable by predictive equations.

The molecular diffusion coefficient and solubility of O_2 in seawater are fairly well constrained (Himmelblau 1964, Broecker and Peng 1974, Garcia and Gordon 1992). If the radius of electrode can be measured experimentally or pre-determined from construction, only the number of electrons involved in a particular reaction must be investigated to arrive at a reliable analytical solution that can resolve accurate bulk concentrations of the electrochemically active species.

1.2.2 Photochemical Sensors

For several decades it has also been practical to resolve in situ DO with photochemically driven optical approaches. Though not the direct subject of this investigation, *Opt*-odes as they're commonly termed, were used for comparisons to the RDEs under evaluation. While they've become the oxygen sensor of choice for AEC, they've have also been a ubiquitous field sensor used regularly in situ for several decades.

Optodes come in a wide variety of formats and utilize the photoexcitation of a specific metal complex embedded in a thin sensing membrane that allows ambient oxygen to diffuse to those sensing sites. In this approach, the metal complex is brought to a higher energy state by an internal light source supplied through a fiber optic cable or window. The complex then becomes unstable and quickly emits this excess energy by fluorescence, an emission of visible light. These photons travel back through the fiber optic cable or window to be measured at a detector. When these complexes fluoresce in the presence of oxygen a fraction of energy that would have been emitted as light is instead quenched or 'absorbed' by molecular O_2, lowering the amount of energy seen at the detector. As oxygen concentrations go up, the magnitude of quenching grows and the emitted signal becomes reduced proportional to the partial pressure of O_2 (ρO_2) in equilibrium with the membrane. Rather than quantifying

an absolute magnitude of photons, optodes are designed to measure the 'lifetime' of emission, τ, or the amount of time until the measured intensity decays below 1/e. Oxygen concentrations are then derived according to the Stern-Volmer relation (eq 3) which equates pO_2 at the membrane surface with fluorescence lifetime and a constant.

$$pO_2 = \frac{\left(\frac{\tau_0}{\tau} - 1\right)}{K_{SV} K_H} \quad (3)$$

Since the Stern-Volmer relationship is non-linear, the calibration of optodes is not as straightforward as that of electrodes. The raw signal response of optodes is to the partial pressure of O_2 across its membrane not directly to bulk aqueous concentration. While Henry's law, $[O_2]_{Bulk} = K_H\, pO_2$, allows one to arrive at a bulk concentration, Henry's constant K_H is itself dependent on temperature and ionic strength. In addition, both the τ_0 measurement and Stern-Volmer calibration constant (K_{SV}) are temperature dependent. Because of these dependencies, the response can be biased by temperature shifts common to many naturally turbulent settings, where improper corrections can lead to large inaccuracies. Increasing pressure also decreases the overall response of optodes, with individual sensor pressure compensation coefficients being poorly known (Uchida et al. 2010).

The more robust optode designs, such as the common commercial Aanderaa optode, utilize large (1 – 3 cm^2) sensing windows or 'foils' with durable silicone

membranes over the sensing material for physical and photic protection (Tengberg et al. 2006). While considered "reliable" for extended deployments (weeks – months) these and similar large optodes tend to exhibit slow response times (60 – 95 s unflushed sensors, Bittig and & Körtzinger 2017), signal drift, and are too bulky for sub-decimeter scale spatial resolution.

To measure at finer space and time scales, optical fiber-based microoptodes with tips commonly 400 - 800 μm in diameter are used both in water column and sedimentary settings (Gouin et al. 1997, Holst et al. 1997, Chipman et al. 2012). While these sensors are relatively stable over short deployments (1 – 3 days), their performance will decay over time proportional to the number of excitation measurements. Thus, high frequency sampling as required for applications such as AEC, shortens their functional lifespan, compromising data quality after only a few days of intense use. These small microoptodes also bear similar issues of breakage to the morphologically analogous glass capillaries of microelectrodes. Even the best attempts to protect microoptodes still require some exposure of the fragile fiber optic core. The small sensing area and lack of the protective silicone layers viable for macrooptodes, also make them much more susceptible to photobleaching, wherein the photoactive sites used for detection in the sensing window's membrane degrade over time and loose sensitivity as a result of both the internal excitation source (Berg et al. 2016) and solar irradiation.

Optode development has largely progressed toward slower more reliable sensors that reduce long term drift for moored or Lagrangian deployments, and have come to a somewhat unified type of sensor widely applied across disparate observing programs in the global ocean (Körtzinger et al. 2005, Bushinsky et al. 2016, D'Asaro and McNeil 2013, Bushinsky and Emerson 2015). This uniformity is useful and can allow for standardized procedures for correction of drift and offsets with in situ air calibrations or post hoc climatological considerations (Takehashi et al. 2013, Bittig & Körtzinger 2015, Johnson et al. 2015). Recent attempts at refinements of the microoptode format (Berg et al. 2016) have tried to push the limits of response times and the ease of submersible deployment, though $t_{90\%}$ values still seem to stall at a floor around ~0.5 s. This limit is possibly a consequence of the thin stagnant boundary layer at the sensing surface, or of the fluorescence lifetime property of optodes which is exploited to make measurements.

Because an optode's excitation and quenching process does not directly consume oxygen, there is no oxygen gradient generated at the sensing surface. As a result, the overall response of the sensor is limited by the time it takes for the membrane system to equilibrate with the external pO_2 (Bittig et al. 2018) which depends on physical properties like the membrane thickness. This

contrasts with electrochemical determinations which, in consuming O_2 directly, produce a gradient at the sensing surface that must be renewed with new analyte at a constant rate to reach a stable and 'accurate' steady state signal. Irregular or sporadic delivery of bulk solution to the sensor, such as may occur during unsteady flow situations, can create false signals termed "stirring effects" reported as problematic in some applications such as microprofiling and eddy covariance (Gust et al. 1987, Holtappels et al. 2015, Reimers et al. 2016). Proper understanding or control of the hydrodynamics at and near the sensing surface of these electrodes is thus crucial to reliable determinations of DO made with electrochemical approaches under non-steady flow present in most every natural setting. Minimizing and understanding the boundary layer thickness at sensing surfaces are also inseparable from flow considerations and important in pushing the limits of sensor response times. These considerations and others prompted an investigation of hydrodynamic electrodes and their behavior in non-steady flow conditions.

1.2.3 Oxygen reduction at electrodes

The reduction of molecular oxygen on Pt metal (often termed ORR) is one of the most exploited electrochemical processes employed in sensing and catalysis applications. While different sensing materials have been developed for the electrochemical determination of O_2 (Wang 2005), cathodic reduction on Pt has seen the most extensive investigation and application through a diversity of communities including environmental systems applications (Kanwisher 1959, Revsbech and Ward 1984, Oldham 1994, Santegoeds et al. 1998, Hutton et al. 2008), to commercial uses in chemical production and automotive engineering. Unfortunately, as in most all multi-electron electrochemical reactions, many of the exact mechanisms and surficial processes involved in the overall reaction series have remained elusive (Katsounaros et al. 2013). However, a generally-accepted scheme with two reaction pathways for non-acidic aqueous solutions has persisted (Pletcher and Sotiropoulus 1993):

$$O_2 + 2H_2O + 4e^- \rightarrow 4OH^- \quad (5)$$

$$O_2 + 2H_2O + 2e^- \rightarrow H_2O_2 + 2OH^- \quad (6)$$

$$H_2O_2 + 2e^- \rightarrow OH^- \quad (7)$$

This scheme includes a slower $4e^-$ reaction (5) combining water and oxygen, and a two-reaction pathway with H_2O_2 as a suspected intermediate (6, 7). The formation of measurable H_2O_2 seems to be more pronounced on non-Pt catalysts

(Wang 2005, Shinozaki et al. 2015). The persistence of H_2O_2 is also driven by the availability of Pt sites on the electrode and mass flux to the active surface, both molecular diffusive and advective (Pletcher and Sotiropoulos 1993). While adsorption of halides is understood to crowd active sites (Katsounaros et al. 2013), the rate of mass flux to and away from the electrode surface has been shown to have a much stronger influence on signal current (Pletcher and Sotiropoulos 1993). Even though not all H_2O_2 generated at the surface is resolved to hydroxide (7), the electrode response remains linear over typical [O_2] ranges for natural waters as long as the mass flux is steady (Pletcher and Sotiropoulos 1993, 1996, Sosna et al. 2007).

Often sensor approaches that employ O_2 reduction on Pt use protective membranes to reduce the fouling of working surfaces, thus extending the working lifetime, and improving signal stability for repeated use (Carritt and Kanwisher 1959, Pletcher and Sotiropoulos 1996). Membranes may be directly coated on electrode surfaces or separated by a layer of electrolyte solution. The addition of a membrane changes the dynamics of reduction at the protected working electrode and adds response-time dependences on the diffusion coefficient for oxygen over that membrane at a given temperature. Common membrane materials like Teflon are only gas-permeable, and do very much improve longevity and stability. However, unshielded membrane-free electrodes

can offer some unique advantages. Used in situ most routinely in sediment applications where matrix flow is negligible (Brendel and Luther 1995, Taillefert et al. 2000, Ma et al. 2008), their translation to water column measurement has largely been limited to research trials with flushed cells (Atkinson et al. 1995, Moore et al. 2007, Sosna et al. 2008) and limited studies in near field hydrothermal vent plumes (Rozan et al. 2000, Luther et al. 2001, Mullaugh et al. 2008). The lack of a membrane affords less encumbered transport of analyte to the sensing surface, decreasing the response time greatly. It also eliminates the pressure effects of membranes (Atkinson 1996), but clear trade-offs do exist with fouling of the surface by biofilm growth, the inevitable intrusion of impurities onto and into the sensing material (Shinozaki et al. 2015), and long term dissolution of the electrode surface to the bulk solution.

1.3 Hydrodynamic electrodes

Forced flow electrodes, also called hydrodynamic electrodes, use a rotating disc or pumped flowline to rapidly and uniformly move solution past a sensing surface (Bard and Faulkner 1980). A common format, the rotating disc, consists of a planar electrode centered at the tip of a rotating shaft (Figure 1). The shaft's rotation forces the thin layer of solution that's at the electrode surface to be thrown radially away from the center, moving tangentially to the electrode surface. The resulting pressure gradient draws in fluid perpendicular to the planar surface and rapidly '"flushes" the area above the sensing surface and its now very thin boundary layer. The faster the electrode spins, the faster the flow toward the electrode and the thinner the boundary layer becomes. The forced mass transport to the sensing surface overcomes the inherent response lag created by the much thicker stagnant boundary layer that exists around every immobile sensor over which O_2 must diffuse to be detected.

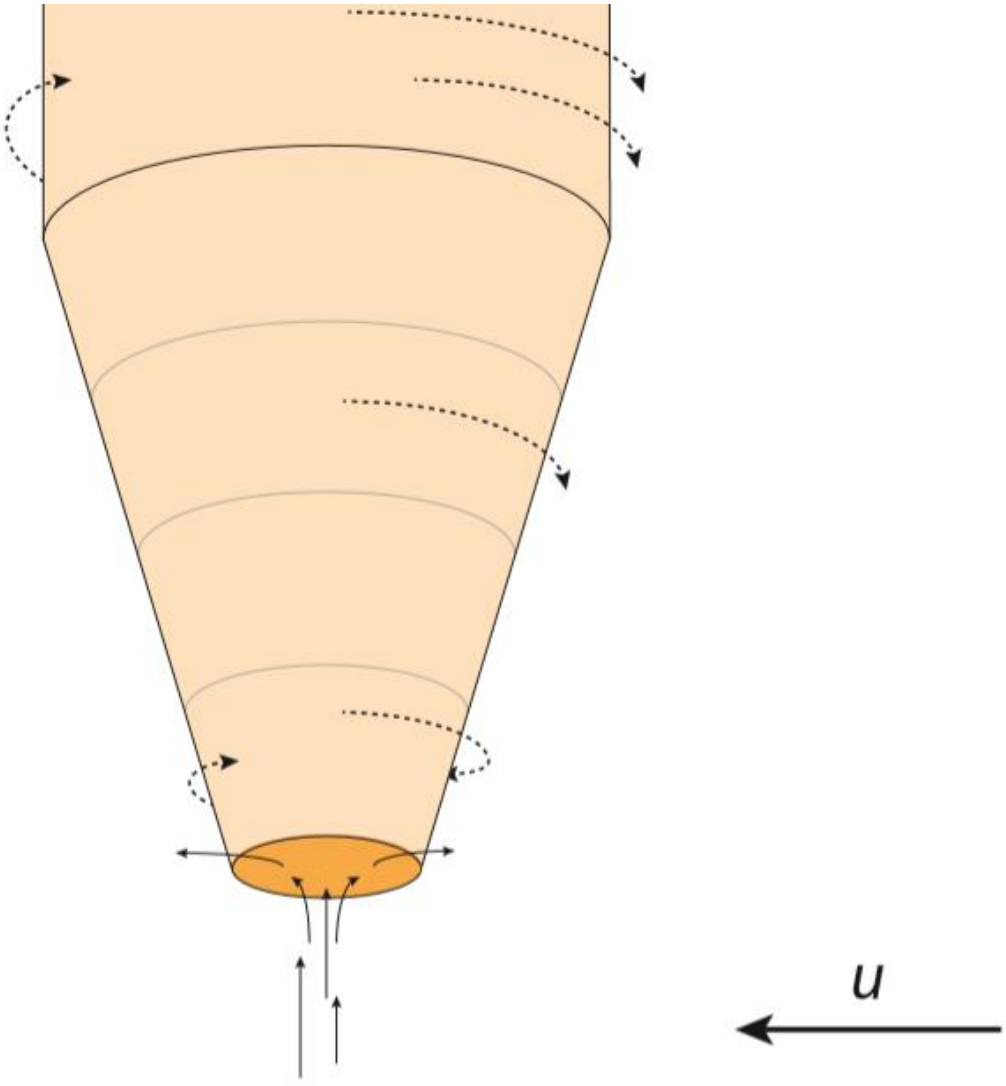

Figure 1. Idealized fluid flow (solid arrows) near the head of a rotating electrode showing the direction of rotation (dashed arrows) in a larger flow field, *u*.

Hydrodynamic electrochemistry has a long history as a benchtop analytical tool using a variety of electrode materials tailored for the detection of a diverse set of electroactive solutes (Bennett et al. 1915). Its chemical principles and governing hydrodynamics have been well defined for some time (Levich 1962) and while used occasionally on seawater samples (Riso et al. 1997, Bruland et al. 1985) and in some very limited shipboard flow-line attempts (Wang and Ariel 1978), no truly in situ applications have been reported. The increased rate of mass flux forces more reactant to the sensing surface, which drives higher rates of transformation, and generally higher signal magnitudes. This increase has been demonstrated with discrete seawater samples to lower limits of detection for some trace analytes like copper (Zirino et al. 2002) and iron (Mikkelsen et al. 2006).

$$i_L = (0.620)nFAD^{2/3}\nu^{-1/6}\omega^{1/2}C \qquad (4)$$

The signal current generated by reactions at a rotating disc is termed the *Levich* current (i_L). This current can be defined by the generalized Levich Equation (4), which encompasses the area of the sensing surface (*A)*, number of electrons involved (*n)*, the analyte's diffusion coefficient (*D)*, kinematic viscosity of the surrounding solution (*ν)*, and the angular velocity of the rotating surface (*ω)*. The rotational term is equivalent to the 'flow rate' term used for stationary surfaces bathed by a solution in fixed flow cells (Wakabayashi et al. 2005, Levich 1962). In equation (4) rotational velocity has units of radians per second while most rotation is measured in revolutions per minute (RPM). It should be noted that the

two are easily relatable by a constant, (1 rad/s = 30/π rpm) though both units are used throughout this study.

A rapid analyte transport to an electrode surface will lead to faster response times for electroactive species with sufficiently fast kinetics, such as oxygen, and it increases the overall volume of bulk solution the working surface comes in contact with. This forced contact with the bulk solution allows more analyte to bind to the working surface in deposition-dependent forms of detection such as stripping analysis for trace metals. In these cases, the increased mass of analyte bound to the electrode, when stripped off, gives an increased signal magnitude. Often benchtop rotating electrodes are employed in small glass vessels of known volumes where purging of gases like N_2 or standard additions can be performed in tightly controlled conditions. Analyses of many oceanographically relevant species require these sample alterations in controlled conditions for appropriate resolution via RDEs. While some approaches reported can forego any sample pre-treatment (Mikkelson et al. 2006), the possibility of deploying an in situ RDE even with some in situ sample treatment in a pre-loaded vessel (acids, etc.) seems technologically within reach and potentially useful in qualitative applications.

1.4 Research Objectives:

The central goal of this work was to investigate the behavior and efficacy of a rotating microelectrode as an in situ chemical sensor, specifically for O_2 in seawater. To date, no reported studies have examined the behavior of any rotating electrode when exposed to the ambient flow fields present in natural waters. The initial interest was in the hydrodynamic benefits of rotating electrodes in producing fast response times (<0.5 s) and potentially spinning quickly enough to overcome the signal artifacts generated from "stirring effects" of natural fluid motions at the electrode. Ideally, a high rotation would produce the steady state conditions met with similar sensors in uniformly pumped flow cells. Understanding this to be a first order investigation of in situ RDEs, there was a focus on four main avenues of evaluation for the O_2-reducing Pt RDE developed in this study:

1. Adapt an electrochemical procedure with reproducible linear responses to DO in seawater able to maintain activity over many hours.
2. Evaluate the response time of a Pt-O_2 RDE (r = 50 μm) in seawater.
3. Evaluate sensitivity to ambient flow conditions (stirring artifacts).
4. Construct and deploy a submersible RDE system.

2.0 Materials and Methods

2.1 Mechanical preparations

Rotating disc microelectrodes (microdiscs) were constructed by sealing 100 μm diameter Pt wire in non-conductive epoxy (West System 105/205). Custom-made pieces were fabricated from nonreactive plastics (polyoxymethylene, 'acetyl,' or polyether ether ketone, 'PEEK') as 'heads' with hollow cores to receive the wire (Figure 2). Before potting, wire was soldered to an electrical contact at the base of the piece, the opposite side of which made electrical contact with the rotating shaft when in place. Excess wire was trimmed and the tip ground and polished with a series of large grit and subsequent diamond polishes (Buehler: 15, 6, 1, 0.25 μm) until displaying a mirror finish (Figure 3). This polishing was followed by vigorous washing with deionized water (Millipore). Individual tips were mechanically prepared and then connected to a shaft for subsequent electrochemical treatment. Head diameter was not varied at this stage of development, but is a property to be reduced in future studies.

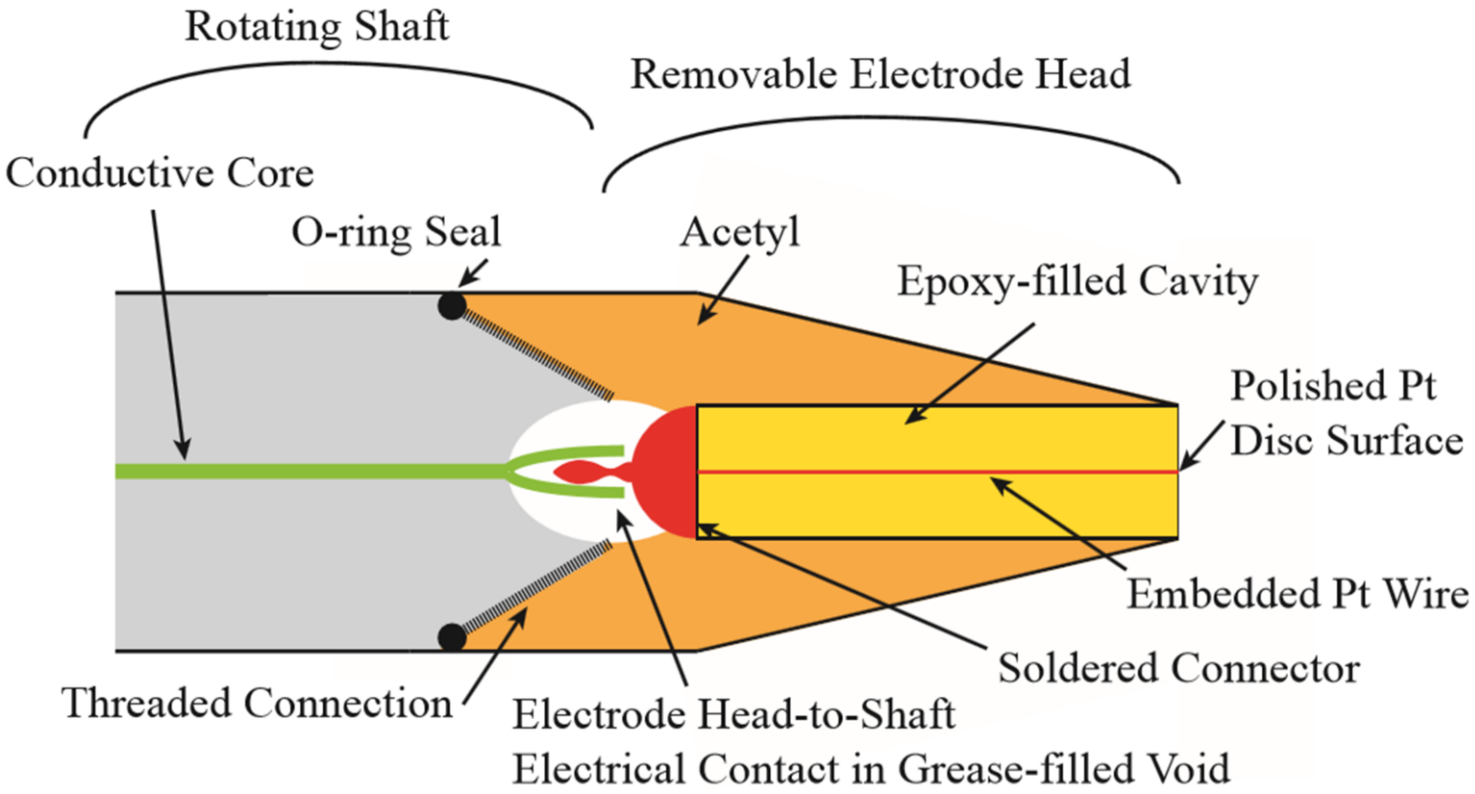

Figure 2. Diagram of the custom-built removable electrode head. The head itself is 4.5 cm from the disc surface to the O-ring seal, and tapers from a 7 mm diameter at the tip to 12 mm at the shaft.

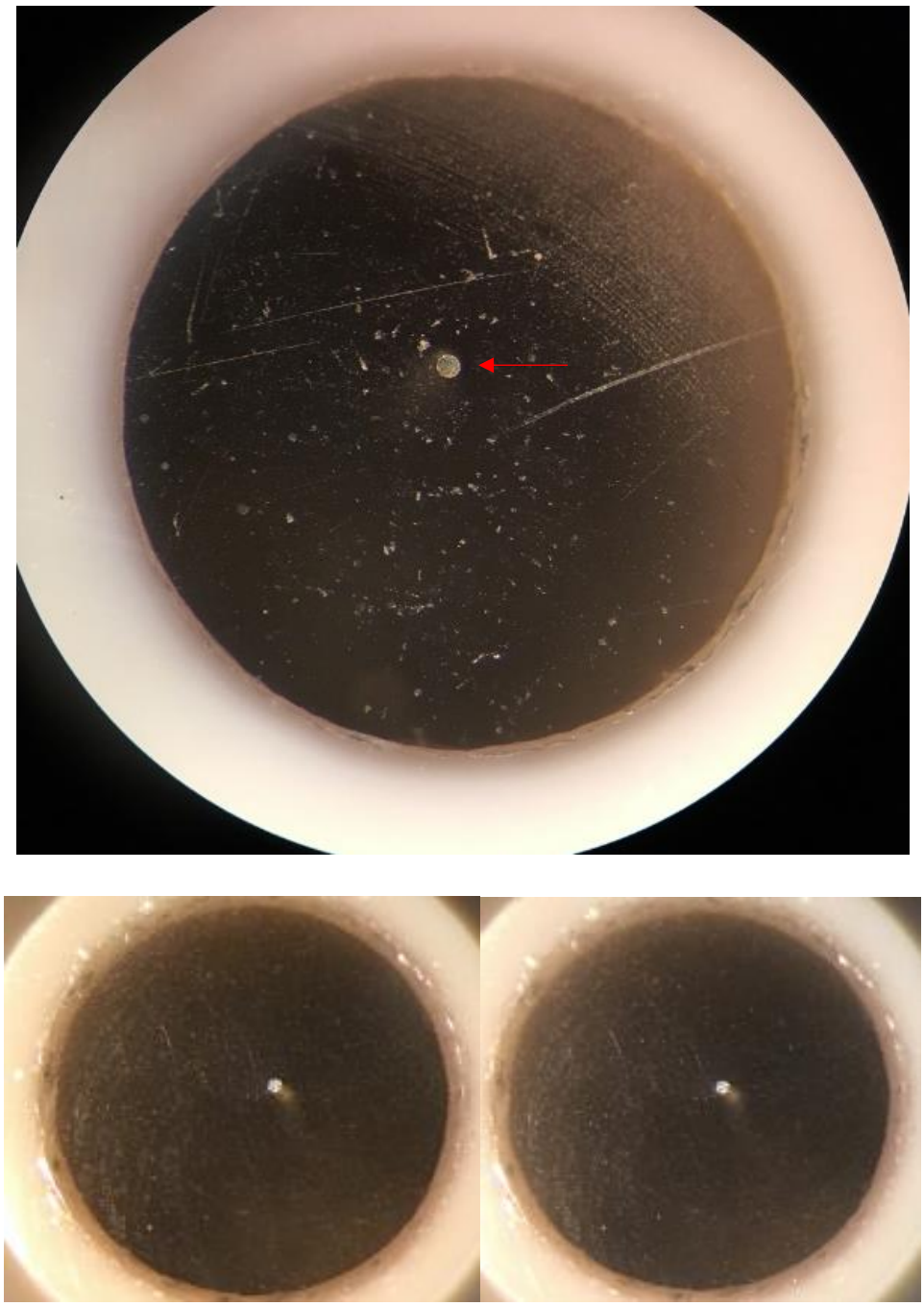

Figure 3. Images of polished Pt surface under x 50 magnification. Disc is 100 μm in diameter (indicated by red arrow), surrounded by epoxy fill which in these images has a diameter of 4.4 mm.

Figure 4. (top) Custom electrode head (Pt disc, r = 50μm) attached to a Pine Research rotator shaft. Tip is 4.5 mm in diameter, tapering to 12 mm at the white sleeve shown. (middle, bottom) Attachment of custom tip to commercial rotator shaft.

2.2 Electrochemical treatments and instrumentation

Electrochemical measurements were driven by a DLK-70 WebPstat potentiostat (AIS; Flemington, NJ). A three electrode system was employed for all tests and chemical treatments, consisting of a working cathode (Pt disc, r = 50 µm), reference (Ag/AgCl in 3M KCl), and large counter anode (Pt wire, r = 250 µm, length > 1 cm). Many assessments of the rotating approach in this study utilized a commercially available benchtop rotator from Pine Instruments (MSR, Modulated Speed Rotator). A standard 12 mm shaft from Pine was purchased and fitted with the removable tips described above (Figure 4**)**. Subsequent assessments of a submersible rotator detailed below utilized electrode heads fabricated exclusively from acetyl and showed no discernable differences from those fabricated in PEEK.

All electrodes, once mechanically polished and cleaned, were put through an electrochemical procedure to both boost their initial activity toward oxygen, and help maintain that activity over multi-day measurement periods. Polished heads were immersed in a bath of 1M H_2SO_4 (Sigma Aldrich) with identical reference and counter configurations. After 5 minutes in the bath to allow passive cleaning of the surface, cyclic voltammograms (CV) were run from +1.25 V to -0.25 V under no rotation (Figure 5). In this simple CV procedure, the applied potential was ‘swept’ from positive, to negative, and back to positive again. This aids in the

removal of impurities bound or embedded at the electrode surface, but also reworks that same surface by encouraging a small amount of dissolution of Pt that is then redeposited in a well-structured pattern. CVs were run on an electrode until a stable, reproducible voltammogram developed, which was usually after 10 – 30 scans performed consecutively and without removal to air.

Various electrochemical procedures were examined to arrive at a reproducible oxygen measurement for this study. Drawing from earlier efforts to develop Pt-based sensors (Pletcher and Sotiropoulos 1996, Sosna et al. 2007) a simple form of chronoamperometry was determined as the best option for the rotating approach. This consisted of an initial brief *conditioning potential* (in this study an oxidative +0.5 V vs. Ag/AgCl) followed by an abrupt "step" to a *measurement potential* that is then held for a longer period of time (-0.75 V for this study). This step between two disparate potentials creates a capacitance or charging current initially present at the beginning of the measurement potential period. This added current masks any true analyte signal initially but quickly decays to allow for accurate analyte determinations (Figure 6). Various lengths of time for both the conditioning and measurement steps were examined to minimize the influence of such charging currents and optimize accuracy of analyte determinations over prolonged measurement periods (hours – days).

Each curve was interpreted individually to extract an electrical current attributable to a specific DO concentration. During benchtop calibrations the steady state signal was examined after the charging effect had subsided and measurements were averaged within a specific 1.0 s interval to extract the single point values shown in subsequent calibration results. All data in this study that isn't a raw signal was extracted using this same averaging of a specific time interval that was kept consistent between curves and within a given experiment. Again ignoring the first few seconds of each curve, averaging over different intervals didn't seem to strongly affect the linear response to oxygen, so long as the same intervals were being compared within each experiment.

On the benchtop under constant DO this averaging method was a fairly straightforward process and appropriate for sensor calibrations. However, once in situ, it was expected the signal in each 12-s chronoamperometric curve would experience abrupt shifts in DO as deviations away from the environmental mean (i.e., as expected in eddy covariance). Signal interpretation was complicated, however, by the fact that the current always decays in a chronoamperometric curve even under steady DO supply. As a result, simply converting the current to concentration with a linear calibration relation was problematic. It was alternatively expected that even if an absolute value was difficult to resolve, the variation of the signal could still reflect real shifts in DO reaching the electrode. In

this case a second well-described sensor (like a microoptode) would be positioned in the same control volume as the rotating microdisc and used to calibrate the RDE in situ.

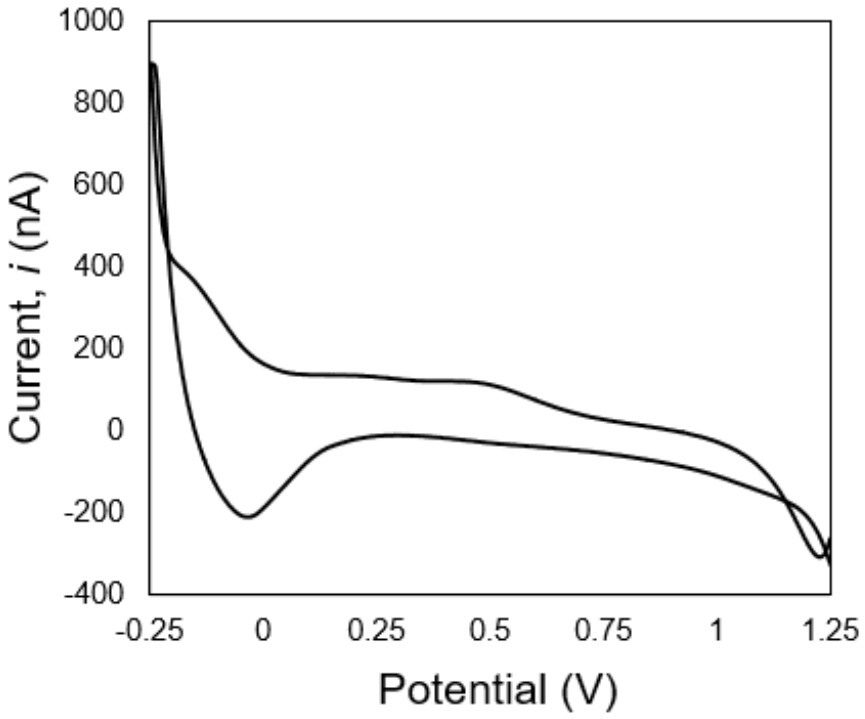

Figure 5. Cyclic voltammogram taken on a Pt microdisc in air-saturated 1M H_2SO_4 prior to measurements in seawater. Such voltammograms were run to maintain activity of the electrode surface and clean it of excess impurities that would show up on the above voltammogram as peaks.

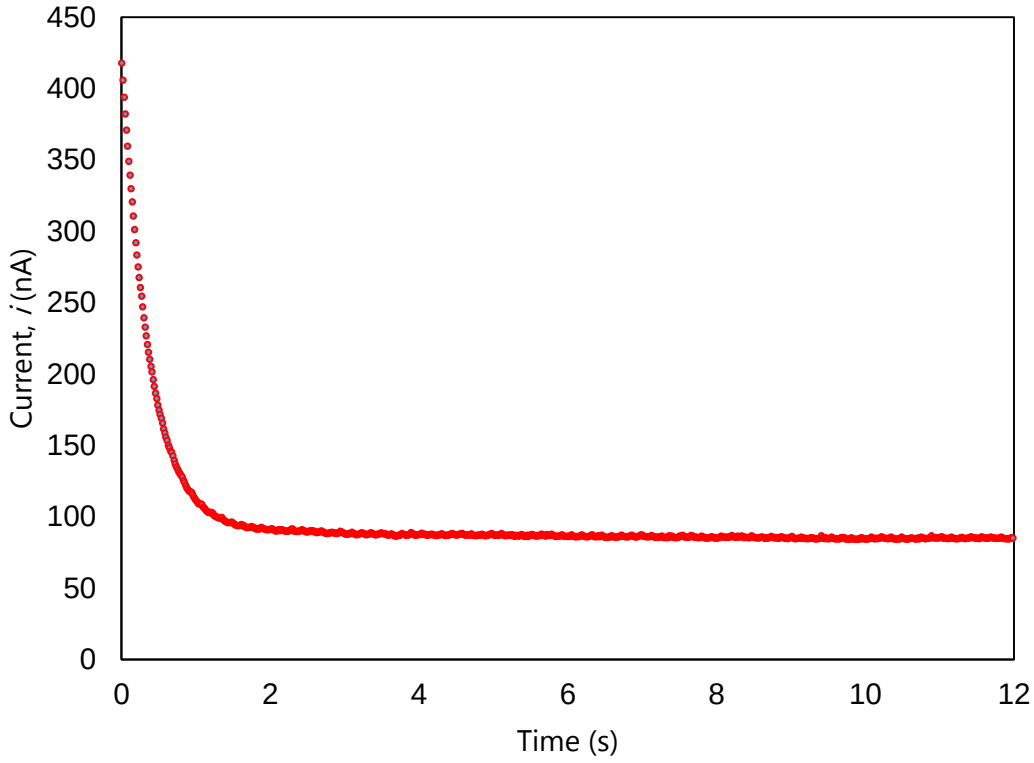

Figure 6. A typical chronoamperometric curve observed using a Pt microdisc in air-saturated seawater (S = 30 psu) at 10.2°C, a 150 rpm rate of rotation, and a 64Hz measurement rate.

2.3 Calibrations and hydrodynamic evaluations

The custom Pt microdiscs made for this study were tested extensively in the laboratory on both the commercial Pine rotator and prototype submersible rotator prior to field trials. The purposes of these tests were to establish calibration characteristics, response times, and interferences or effects created by variable external flow. A MCQ 3-channel B-103 Gas Blender was employed with two stocks of ultrapure N_2 and compressed air (AirGas) to make solutions at standardized [O_2] in filtered (0.2 µm) seawater or river water. Calibration measurements were performed in a glass beaker with a water jacket for thermal control and rubber top gasket to restrict exiting gas flow. Gases were mixed externally and then pumped into the measurement vessel via nylon tubing, both bubbled-in directly with a glass airstone and into the headspace to prevent intrusion of ambient air. The rubber gasket was designed with ports to receive the rotating shaft, counter and reference electrodes, as well as the gas line, a temperature probe, and microoptodes for concurrent calibrations.

Response times were tested separately by passing sensors between N_2-purged and oxic water volumes without removal to the air. This was accomplished using a long track (80 cm long, 8 cm wide) with a gate at its center consisting of two equally-sized doors on springs (Figure 7). Seawater on one side of the gate was purged for a set period with N_2 while seawater on the other side lightly bubbled

with compressed air. The less oxic side was never purged to complete anoxia, only to create a difference in oxygen concentration between sides. During response time tests, the electrode was allowed to equilibrate on one side of the gate, then moved quickly through the doors with them shutting rapidly behind the sensor from spring-action, affording a relatively clean break from one solution to the other without generating a large amount of mixing. The extremely physically durable rotator shaft and tip easily passed through the stiff gate (high tension springs were used for optimal shutting speed). More fragile sensor formats (microoptodes) tested in the same track had to have a partial rigid sleeve covering their main body to prevent breakage during testing.

A second response evaluation was conducted in a 150 x 15 x 15 cm re-circulating linear flume using the commercial rotator. Instead of a clean break between two disparate solutions, the electrode was placed in a ~2 cm/s steady background flow and allowed to reach a steady reading in air-equilibrated seawater. Once steady signals were observed, a small nozzle attached to a vessel of N_2-purged seawater (positioned above the flume and gravity siphon-fed) was placed upstream from the RDE. Anoxic solution was then siphoned into the flume and carried by the flow to and past the RDE, introducing small ‘puffs’ or ‘pockets’ of low oxygen water that could be detected by the sensor.

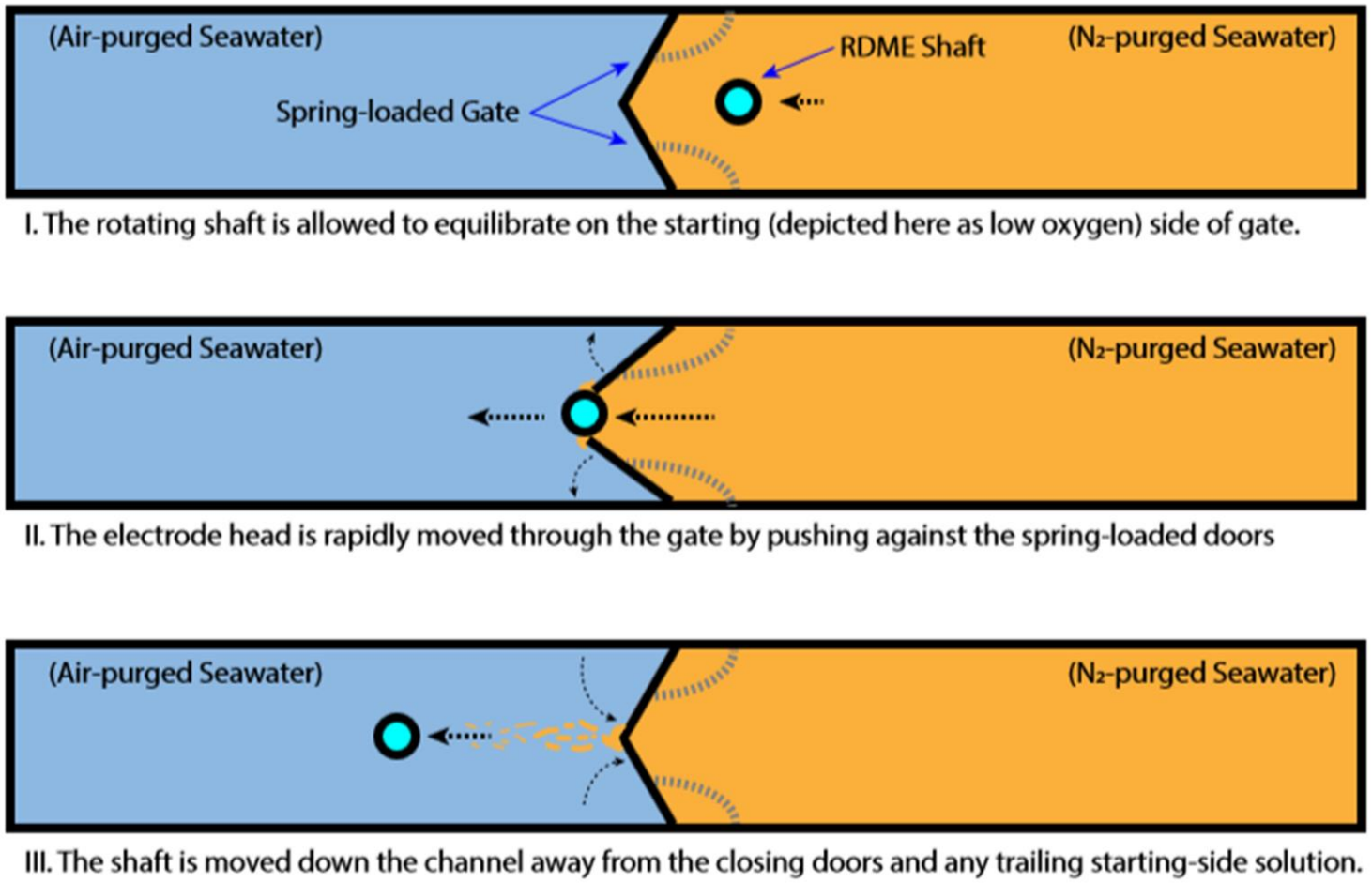

Figure 7. Top-down depiction of response time testing apparatus constructed from a long channel (1 m) with a spring-loaded gate separating seawater volumes of different DO levels.

Additional tests were performed to identify any flow-induced artifacts (i.e. the "stirring effects" seen in capillary microelectrodes). Using the same laboratory flume with no recirculation, the RDE was allowed to equilibrate at one end of the flume at a fixed rotation rate. A single wave motion was then initiated from the opposite side of the flume by manual immersion of a foam wedge into the water, generating a clean wave that would travel down the flume and pass by the sensor. Due to the interruption of the electrode measurements by requlars conditioning (described in section 2.2. and below) and the short travel time of the wave down the flume, these tests did not always produce a consistent wave arrival but were able to show (1) any pronounced wave motion effects that occurred during the measureable signal period and (2) if these effects were dependent on the rate of rotation.

2.4 A Submersible Electrode Rotator

A watertight electrode rotator, WER-I, was designed and constructed following the principles of common laboratory electrode rotators in partnership with the Sexton Corporation (Salem, Oregon) (Figure 8). This prototype device consists of an electrode head, as described above (Figure 2), positioned at the end of a rotating shaft. The shaft itself has a low resistance conductive core that makes contact at its non-electrode side to a low-noise slip ring, affording stable signal transmission under rotation. Rotation of the shaft is accomplished by a brushless DC motor (ElectroCraft, 7.6 amp) driven by an accompanying controller that communicates via USB to a computer running a common interface software Roborun+. Both motor and board are contained in a watertight housing and physically isolated from the sensor signal path, though no additional shielding was employed to isolate the sensor signal from motor noise (magnetic influences) in this prototype.

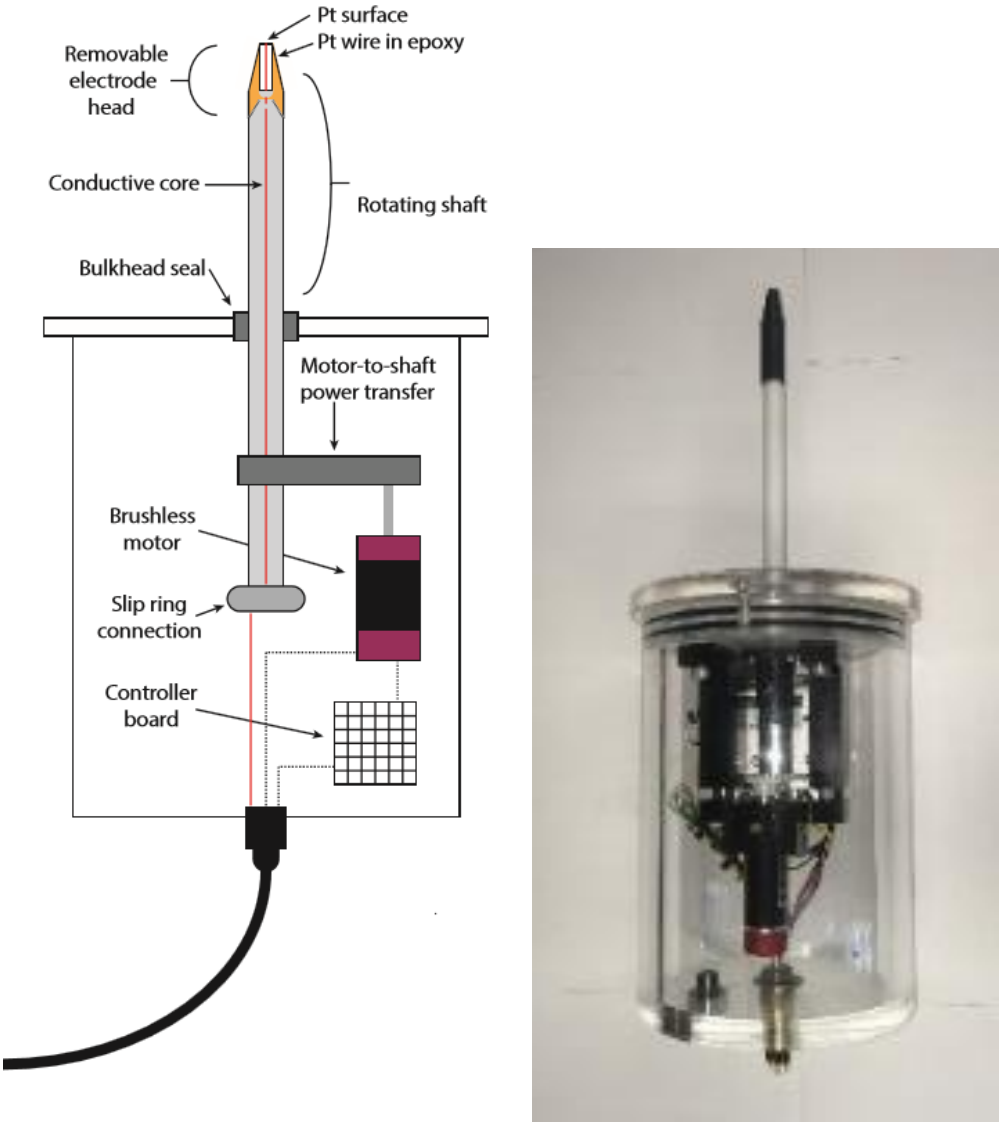

Figure 8. Schematic of the WER-I prototype with photograph of same instrument. Cylindrical polycarbonate housing shown is 15 cm in diameter, and the protruding shaft is 12 mm in diameter, extending 18.5 cm from the bulkhead seal of the pressure housing.

Intended to span a range of shallow water depths (<10 m), the WER-I is the first truly in situ electrode rotator described. The main housing cylinder was not optimized for size and is 15 cm in diameter and 24 cm long, with the shaft extending 18 cm from the main housing. The shaft has a double-wiper seal to prevent water intrusion into the housing, and its internal electrical contacts and paths are isolated from the external solution. The shaft extending outside the housing ends as a male thread with an electrical contact designed to receive the custom electrode tips (Figure 4) containing the working electrode. An additional O-ring seal used at this threaded connection (see Figure 4) prevents water intrusion to the shaft's contacts under rotation and pressure.

The WER-I has a bulkhead connection with 8-pin submersible connector and cable to carry power for the rotator motor and control board, as well as to carry the working electrode signal. The cable is split after 1 m to separate the working electrode signal path, controller communication path, and power lines into isolated cables. When deployed as part of a three electrode system, counter and reference electrodes are run with separate dedicated cables and positioned at a fixed location <60 cm from the rotating head.

2.5 Field deployments

Field trials of the WER-I were conducted in Yaquina Bay, a small drowned river estuary on Oregon's central coast. Its lower reach is marine-dominated with generally high salinities (S >25 psu). Tests were carried out in < 2 m of water depth on flood tides absent of much wave activity. Sites were chosen along the South side of the bay, away from the main channel and strong cross bed flows. Sensors were positioned above a non-vegetated sandy bottom. Three useable deployments were completed. The first was only with the WER-I, which was positioned with its microdisc pointed vertically downward, attached to a small steel frame. The sensor head was ~30 cm above the bed and in a total depth of just above 1 m. No other sensors were included, but measurements of temperature and salinity near the rotator were made regularly during the deployment with a hand-held probe (YSI Pro-30, Yellow Springs, Ohio).

For the second and third deployments, the WER-I was fixed horizontally in the center of a cubic titanium frame 1 meter tall (Figure 9). A microoptode (Pyroscience FireSting) was co-located with the rotating head, with its tip positioned ~1 cm away horizontally from the electrode head so as to not obstruct flow being drawn to the electrode from rotation. Microoptodes were controlled via a Rockland Scientific (Victoria, BC Canada) Microsquid control unit attached to the frame and integrated with a velocimeter (Nortek Vector)

sampling at 64 Hz in a fixed control volume 5 cm away from the rotator head but on the same vertical plane. Also, on the frame were a pair of HOBO temperature and light loggers. Additional point measurements of temperature and salinity were made by wading into the water and lowering the YSI probe within the frame to the vertical height of the rotating sensor during measurements. Counter and reference electrodes were run on independent cables from the shore terminal to the frame, and attached within the frame at the same height of the rotator ~40 cm away.

For all deployments the working electrode was run identically as in laboratory evaluations with pre-deployments calibrations (3-point). The chronoamperometric electrode procedure was run continuously from the start to end of the experiment, but due to the potentiostat used, there were periods of no measurement during “data archiving” steps required by the instrument programming. During these periods the electrode was left to be at open circuit with no set holding potentials.

Figure 9. Images of prototype WER-I on field frame awaiting an incoming tide in Yaquina Bay, February 2019.

3.0 Assessment

3.1 Conditioning and linearity

Various iterations of the chronoamperometric procedure described above were examined. As with prior studies it was found that an oxidative conditioning step was necessary to maintain stable activity toward oxygen over any prolonged period of time. Once the signal stabilized after a few seconds it would continue to decay were no oxidative step re-introduced. This decay will finally plateau after roughly 72 h to a somewhat consistent reading (Figure 10), but the 92% loss of signal magnitude makes an unconditioned Pt microelectrode too insensitive to be used as a reliable sensor. While not a new finding for Pt generally, it was important to verify this in the rotational format and to determine an optimal reduction time to maximize the period of resolvable signal. Ultimately a measurement period of 10 – 15 s at -0.75 V proceeded by 0.25 s at +0.5 V was found to be optimal for maintaining activity over multi-day periods (Figure 11).

Conditioning in H_2SO_4 was also verified as a crucial preparation step to boost electrode activity and maintain signal viability over multi-hour long measurement periods. Conditioning CVs exhibited unidentified peaks indicative of plated and adsorbed material on the electrode surface seen on similar Pt microdiscs when used in seawater (Sosna et al. 2007). It should also be noted that following acid

conditioning, the electrode would have to be run in the described chronoamperometric procedure repeatedly before it reached a consistent measurement. This regularly took 20 to 50 repetitions, but was usually run for upwards of 100 iterations to be sure the response was stable.

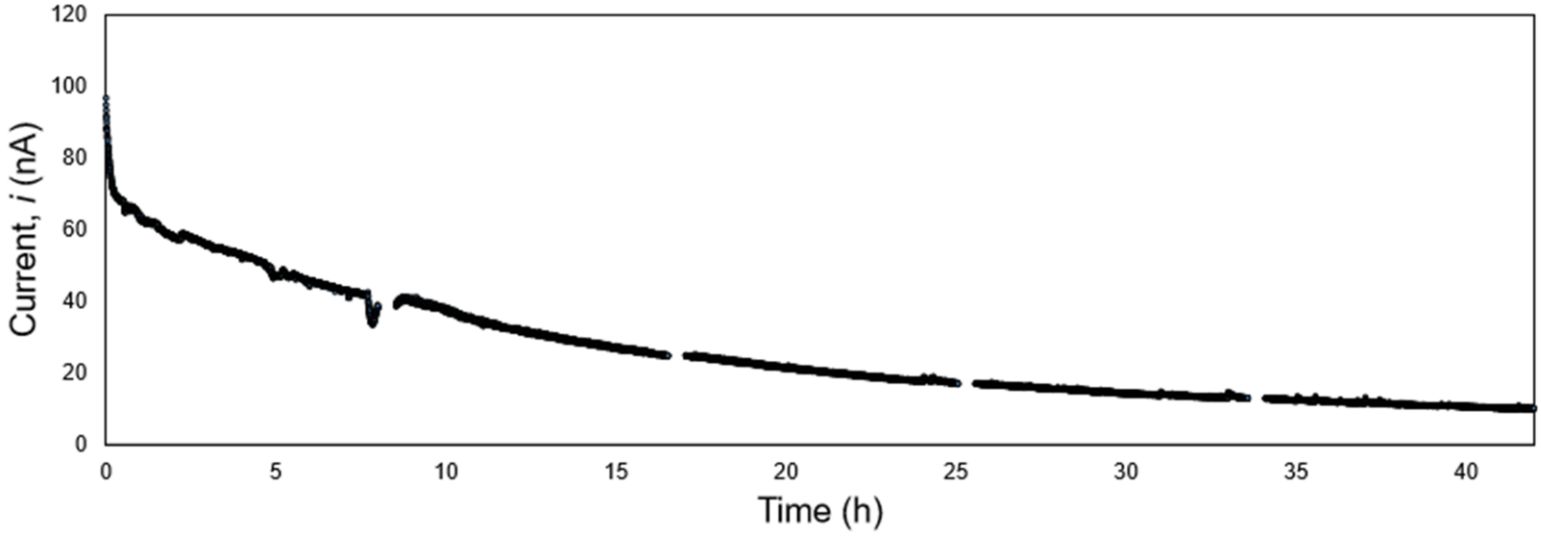

Figure 10. Chronoamperometric curves performed with no oxidative re-conditioning over 48 hours (a) and 8 days (b).

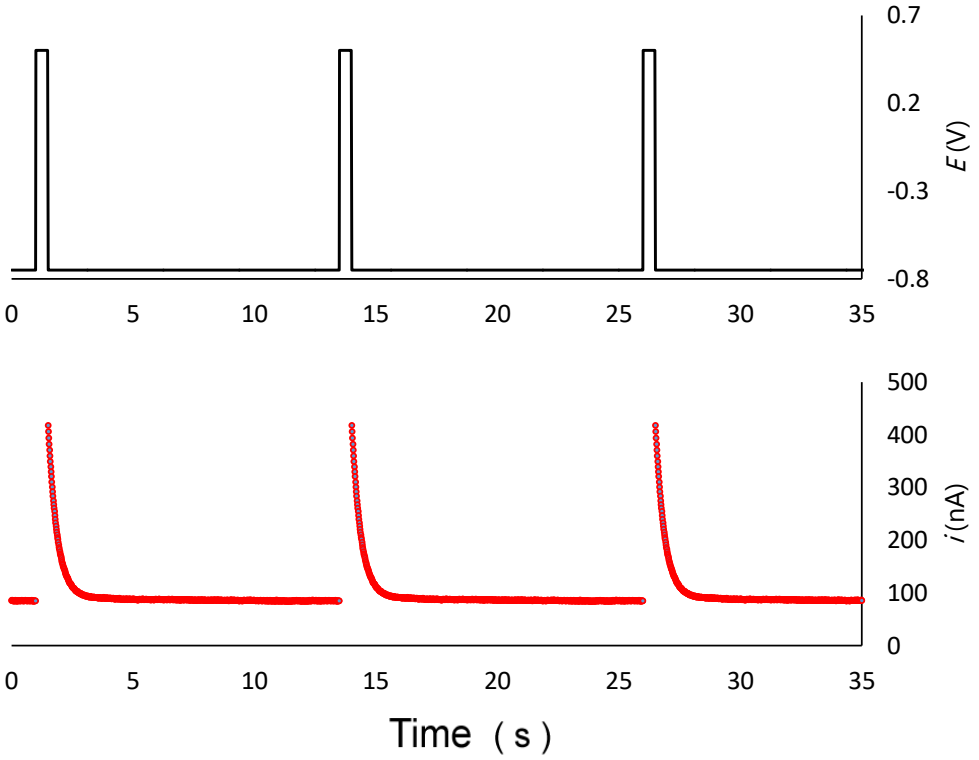

Figure 11. Times series showing the applied potential, *E*, and resulting current output, *i*, from the Pt microdisc. This was the predominant electrochemical procedure applied throughout laboratory and in situ measurements.

The linear range of electrode response to oxygen was also examined. While the linearity of a Pt electrode to oxygen is often taken as a given, this linearity is actually contingent on the type of electrode used, matrix composition, and electrical noise considerations. With multi-point calibrations the Pt disc under rotation was found to exhibit a tight linear response ($r^2 > 0.90$, Figure 12) to dissolved oxygen with a maximum value tested at 285 µM in 35 psu seawater, and 365 µM in filtered river water. This linearity is sure to extend to higher concentrations, but mixtures with oxygen above atmospheric values were avoided because gas mixing with pure oxygen was found to introduce too much uncertainty and variability. Ten percent saturation was chosen as the lower limit for multi-point calibrations to avoid any uncertainties introduced by the gas mixer when mixing at small ratios. While a nitrogen "zero" point was obtained for all calibrations, these points regularly exhibited the highest uncertainty with % standard deviations taken from the most quiescence final seconds of usable signal being as high as 10 - 16 % of total signal, as opposed to a ~ 1.5 % mean deviation seen when oxygen was present (Figure 12).

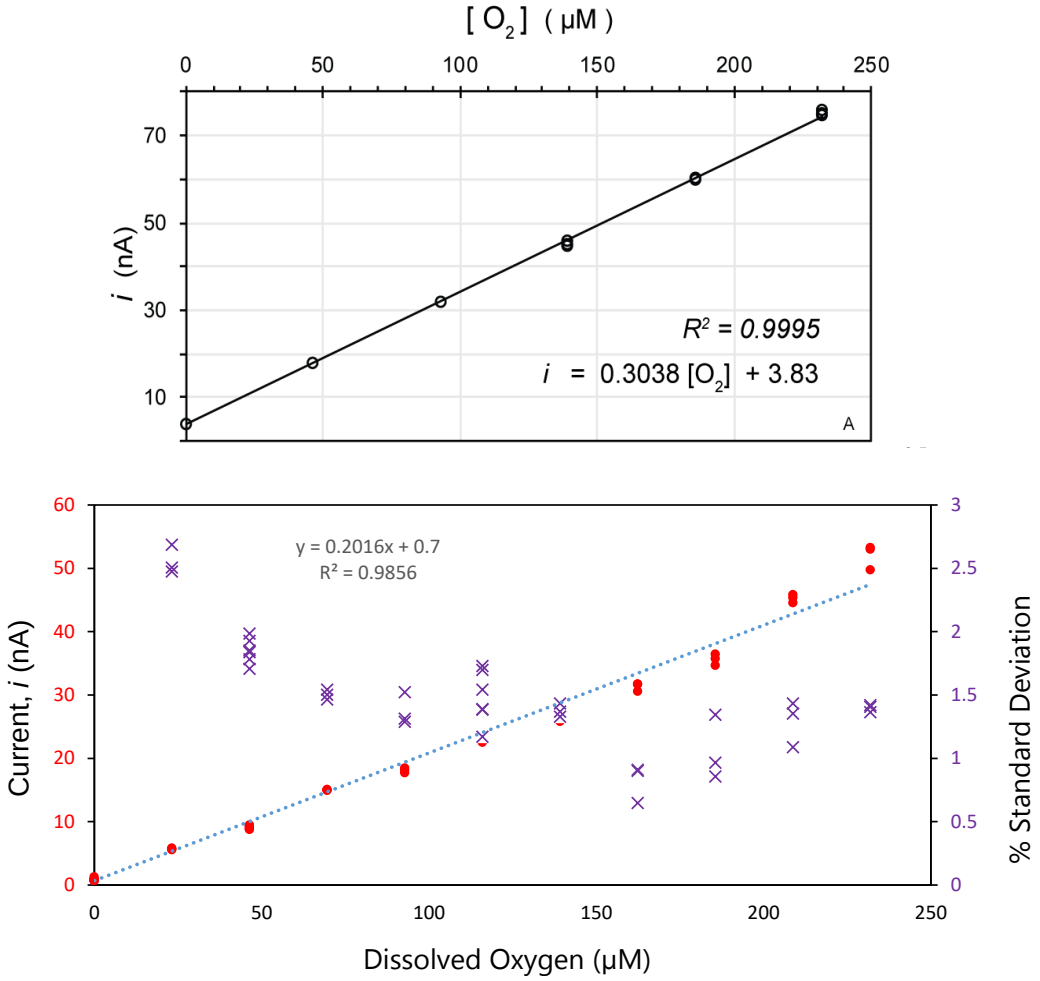

Figure 12. Examples of two different Pt microdisc responses to dissolved oxygen (a) and (b), with (b) showing the % standard deviation which in this case is largely electrical noise. % values for $[O_2]$ = 0 µM in panel (b) were between 10 – 16%.

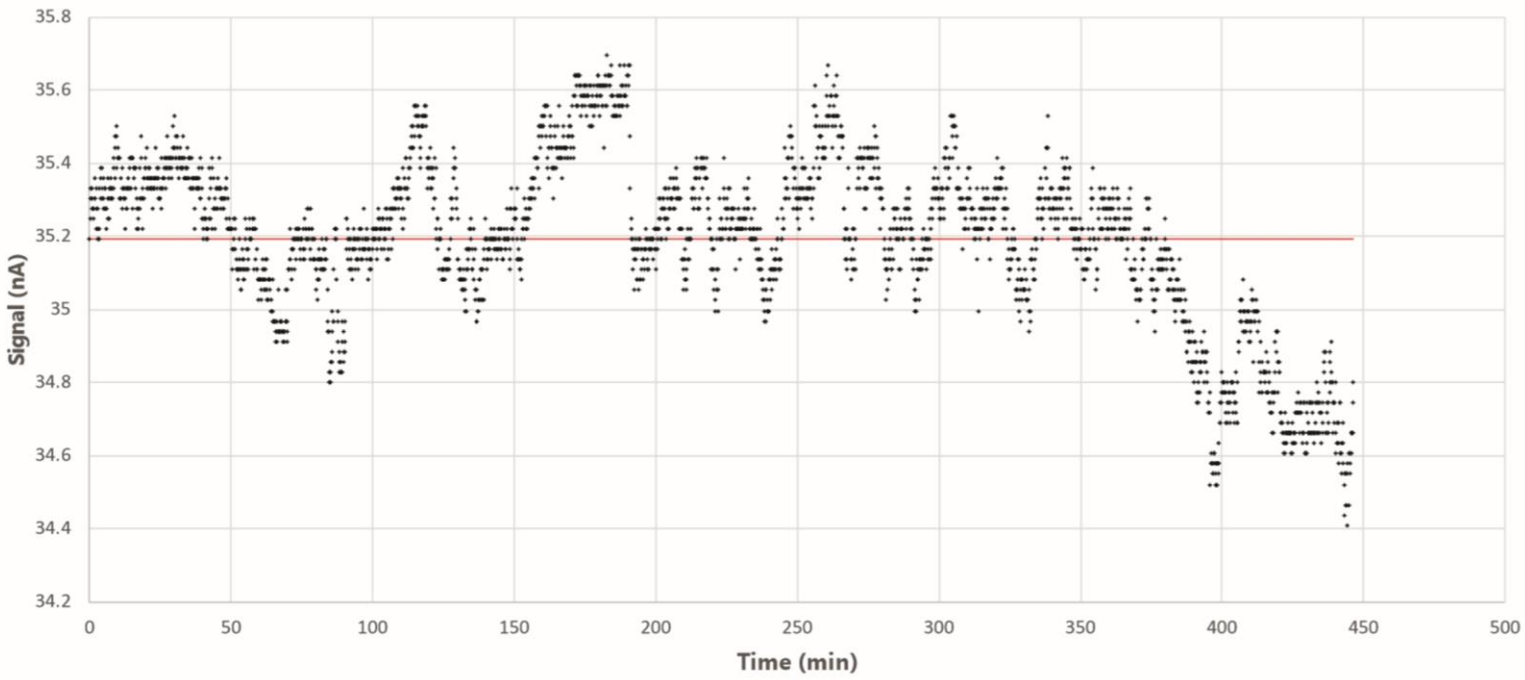

Figure 13. Averaged microdisc outputs measured over an 8 h long experiment in air-saturated filtered seawater (20°C, S = 34) with no variation of dissolved oxygen levels, red line indicated the 8 h mean value. Values were extracted by taking the average of the last 3 seconds of each chronoamperometric curve. A post-run three-point calibration confirmed this microdisc maintained a linear response DO (R^2 = 0.996).

3.2 Matrix effects

While an extremely complex mixture, seawater tends to exhibit a relatively consistent composition in regards to chemical species and properties that can influence the Pt ORR. As such, only major effects from variations in temperature and salt content, or salinity as defined in an oceanographic context, were investigated. Temperature was varied widely (4 – 35 °C) between experimental runs but was kept consistent within the period of measurement (±0.1 °C). Effects were examined by measuring with the same electrode without any mechanical cleaning or acid reconditioning over a day-long experiment where the temperature of the solution was shifted up and down. After corrections for the oxygen solubility at those particular temperatures and salinities the measurements were overlaid with one another and revealed no discernable deviation ($r^2 > 0.95$) from the linearity exhibited by calibrations at a single temperature (Figure 14). Though this can only be said to be verified for the steady state conditions in laboratory measurements.

Salinity was investigated in a similar manner, with a series of filtered seawater solutions diluted with deionized water to various concentrations, and a filtered volume of river water collected from the middle reach of the Willamette River used as the 'zero' salinity value. The ion content of the river water was deemed high enough to act as a sound electrolyte but negligible compared to the much

higher concentration aliquots of seawater. A linear response to DO concentration was found to be maintained in all of these samples (Figure 15). It must be noted that while reproducible calibrations were derived at specific salinity values, salinity was not varied in a complex way during measurements, and it was seen that calibration slopes did decline with less electrolyte in solution. This behavior suggests the response of a bare Pt RDE would be difficult to interpret in environments with highly variable salinity, as with many other DO sensors.

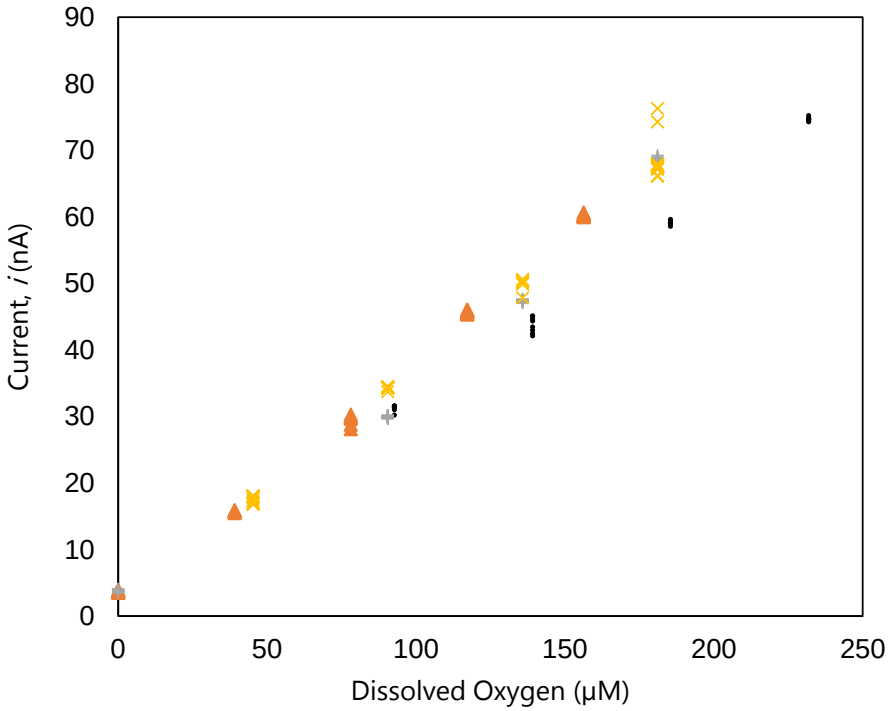

Figure 14. Pt microdisc calibration measurements in seawater (S = 31) at four different temperature values: 35.0 (x), 30.1 (+), 20.1 (Δ), and 10.5°C (•). All of these points taken together have a R^2 = 0.975 and a collective slope of 0.34 nA / µM / at 500 rpm. However, the 10.5°C curve shown did deviate clearly from the warmer measurements, and may speak to temperature effects on reaction intermediates of the ORR like peroxide.

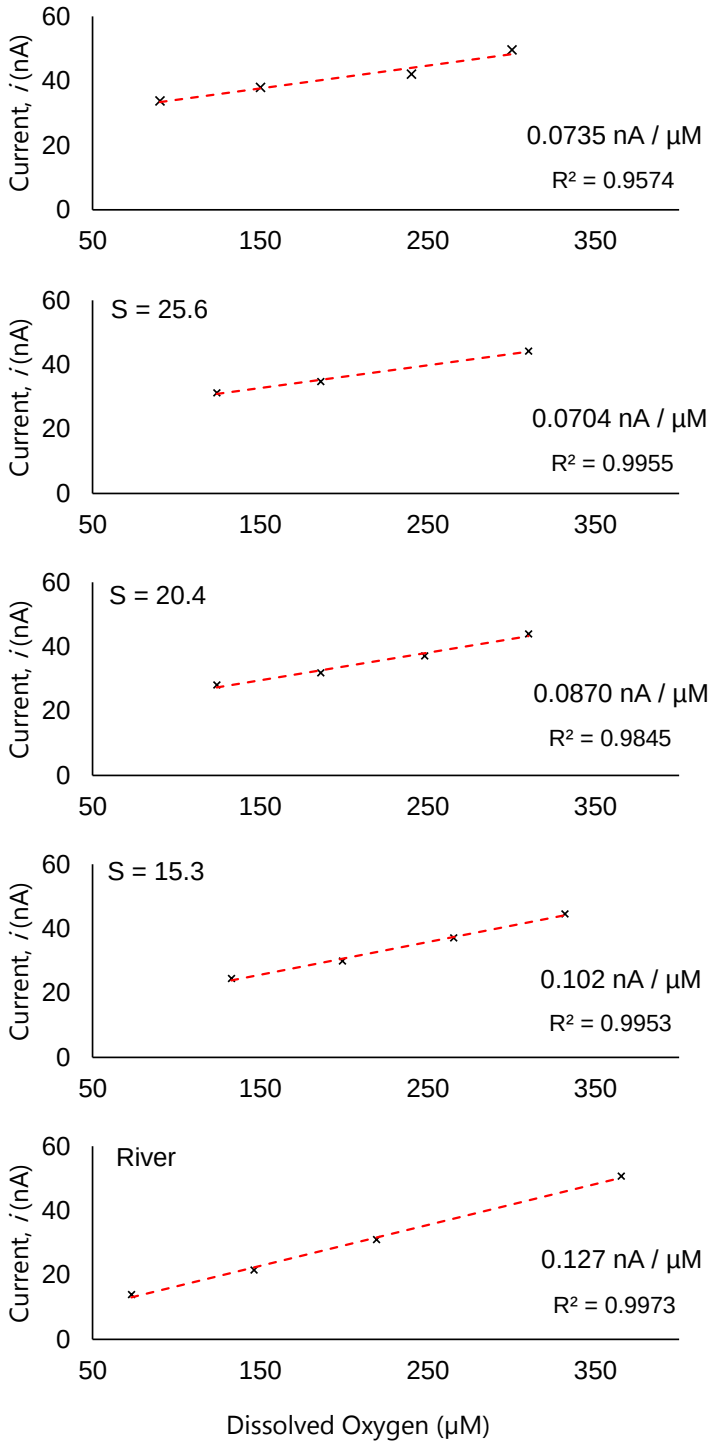

Figure 15. Pt microdisc calibrations in solutions of varying dissolved oxygen and salinities, S (psu), performed under low rotation (30 rpm).

3.3 Hydrodynamic evaluations of rotation rate dependence and response time

Initial tests verified with high confidence that the signal of a RDE was dependent on rotation rate as predicted by the Levich equation (eq 4). This was consistent both for the microdiscs (r = 50 μm) used in the bulk of this study and a commercial Pt macrodisc (r = 5 mm) employed during early experiments (Figure 16). The linearity of the macrodisc (Figure 16a) is particularly useful, as its linear response is evidence that there are no significant heterogeneity influences of reduction across Pt-sites at a rotating electrode surface that should be much more prominent on a disc 3 orders of magnitude larger (Pletcher and Sotiropoulus 1996). Current increased predictively with rotation rate during the previously described flume tests. This was done to examine if there was any the influence of a ~2 cm/s horizontal flow on the rotational dependence of the signal, which was found to still exhibit a tight relationship (r^2 = 0.97, Figure 17).

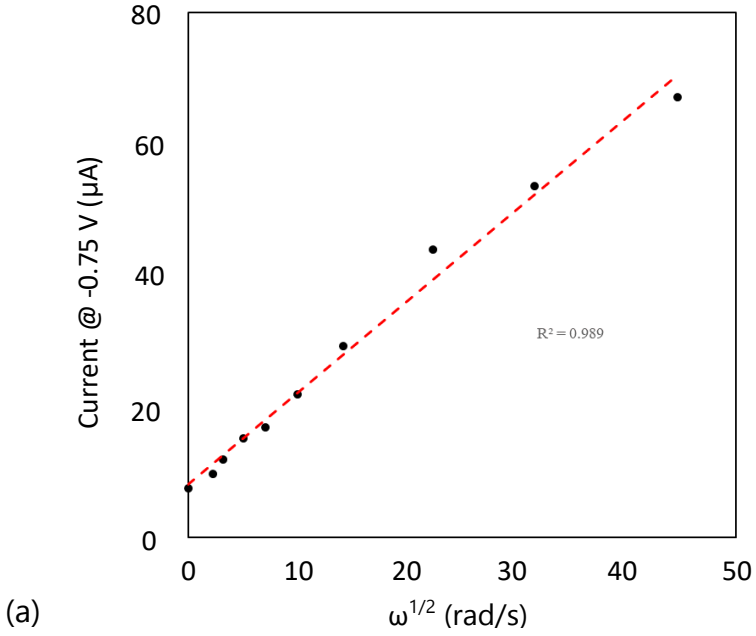

(a)

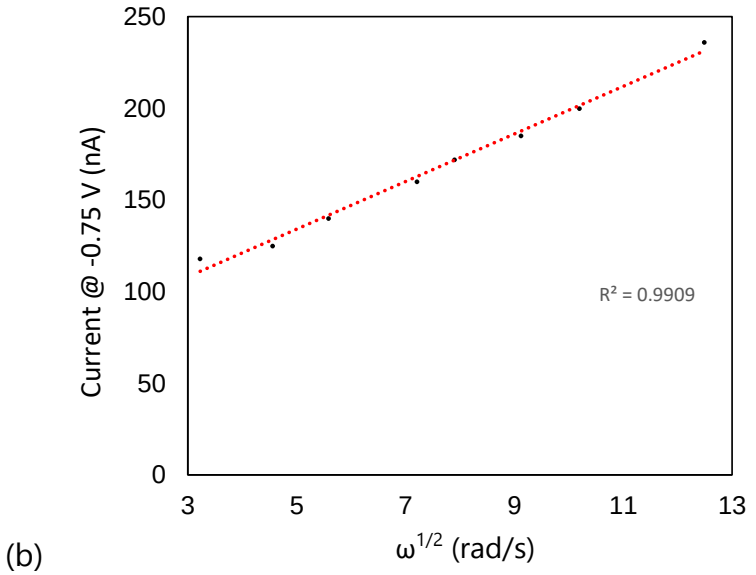

(b)

Figure 16. Oxygen reduction current dependence on angular rotational velocity, shown here in radians per second on (a) a commercial 10 mm diameter Pt disc electrode (Pine Research) (b) and a custom-built 100 μm diameter Pt disc in 0.45 M NaCl solution. Values were electrical current at E = -0.75 V and were obtained by linear sweep voltammograms from +0.1 V to -1.0 V.

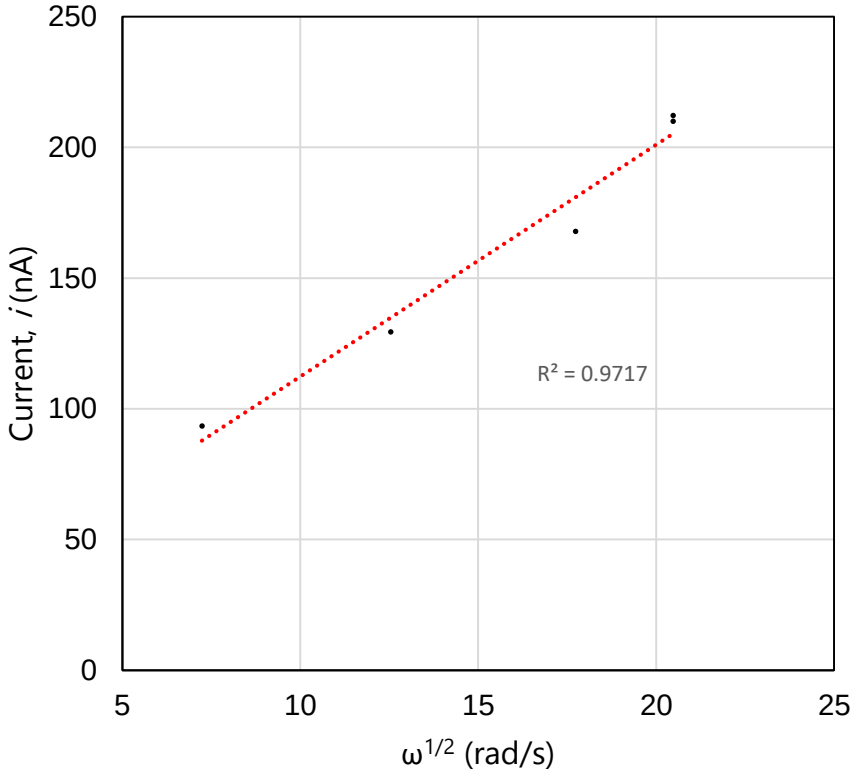

Figure 17. Dependence of *i* on rotation rate in a flume (a) under 2 cm/s.

Measurements are 1 s averages taken from chronoamperometric curves.

Response time evaluations in the gated apparatus used contained a great deal of inconsistencies from human operation, however, it was still possible to reproduce results of fast response times. Overall the fastest response times measured were on the order of $t_{90\%}$ ~ 50 ms (n = 3, 2500 rpm) and generally <100 ms. The RDEs consistently had response times that were roughly an order of magnitude faster than 'fast responding' microoptodes concurrently evaluated (Figure 18). The quality of these responses was shown to be heavily dependent on the presence and severity of electrical noise, which in a laboratory environment outside of a Faraday cage regularly polluted the signal at frequencies comparable to the time scales of interest (see Figure 18c) .

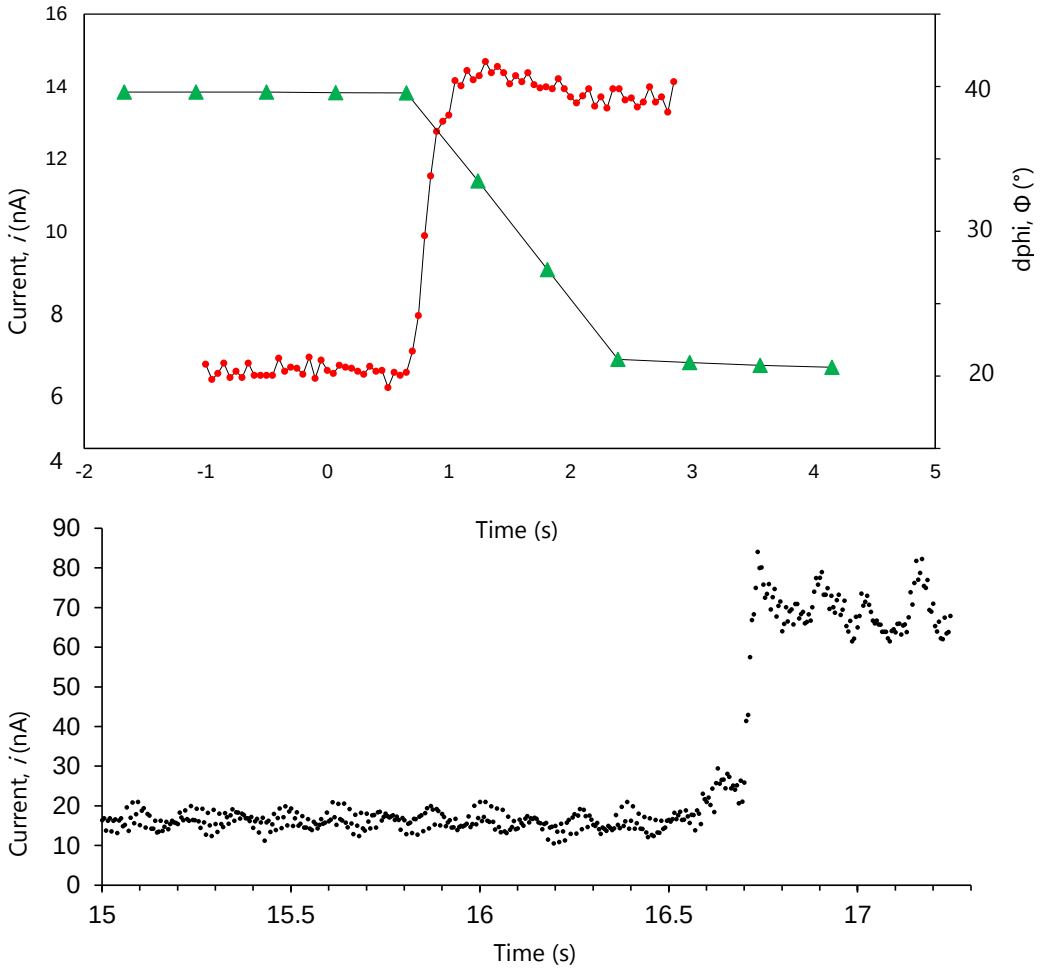

Figure 18. Examples of Pt microdisc responses under rotation to abrupt shifts in oxygen concentration (see Figure 8). Includes (a) test pairing a commercial rotator at 1000 rpm and a microoptode (Pyroscience) tested in tandem, (b) one of the faster RDE response times measured, (c) response of same microdisc performed without any physical shielding or signal filtering. Clear oscillation patterns (c) illustrate the issues of electrical noise regularly encountered with these systems in the laboratory and that noise level increases with the magnitude of output signal.

Further tests in the laboratory flume were undertaken to introduce strong wave motions around the rotating electrode surface in a larger water body and note any anomalies. The most discouraging finding of this work was that wave-induced signals were detected consistently (Figure 19). At lower rotation rates this bias was much more prominent, but there was what appeared to be the hoped for “wash-out” threshold, where the rate of rotation would overcome or be so much higher than ambient motions that those motions would not be significant in the eventual electrode signal. Though this threshold was found to be above 4000 rpm, with the ‘cleanest’ values seen at even higher rates. At these high rates of rotation significant amounts of momentum are also introduced to the surrounding solution.

Further response tests, described as ‘puff’ tests above, performed in a re-circulating flume showed evidence of this rotationally induced external mixing in the sensor response. A stream of anoxic water volume was passed back and forth across the width of the flume upstream from the electrode. Rather than clean breaks as in the gated response tests (Figure 18), smooth rises and falls were seen (Figure 20) that are likely indicative of the eternal mixing induced by the rotating head. As the anoxic stream approaches the rotating head it is mixed externally within the electrode’s own flow field with the surrounding oxic water, producing

the smooth rise and fall rather than a break as seen when passing through discrete parcels.

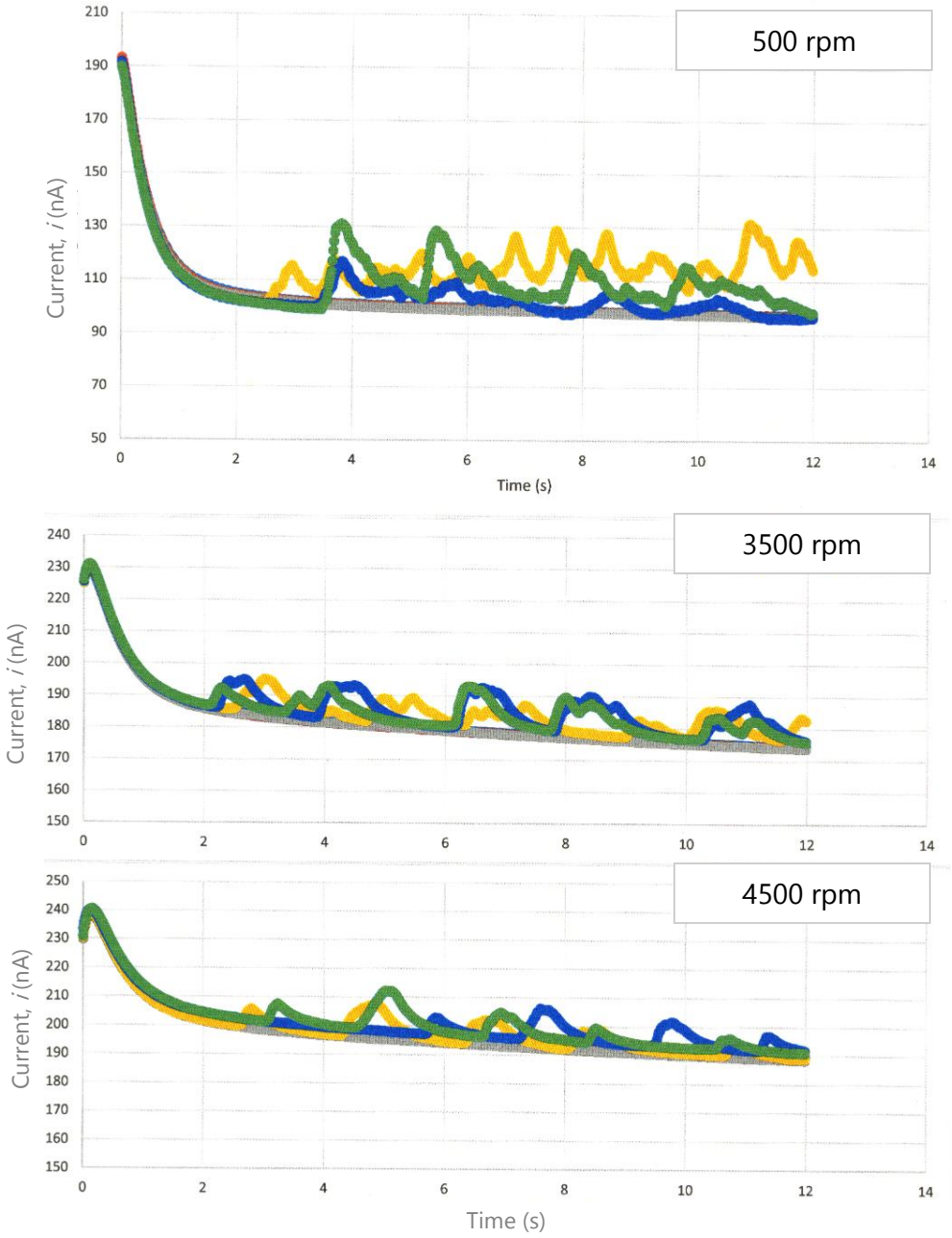

Figure 19 a. Results of 'wave tests' described in methods at increasing rates of rotation (18.2°C, S = 34) using a commercial rotator (Pine MSR). Each color is a different 12 s period of measurement. The smooth 'baseline' curves were taken from measurements just before introduction of the wave.

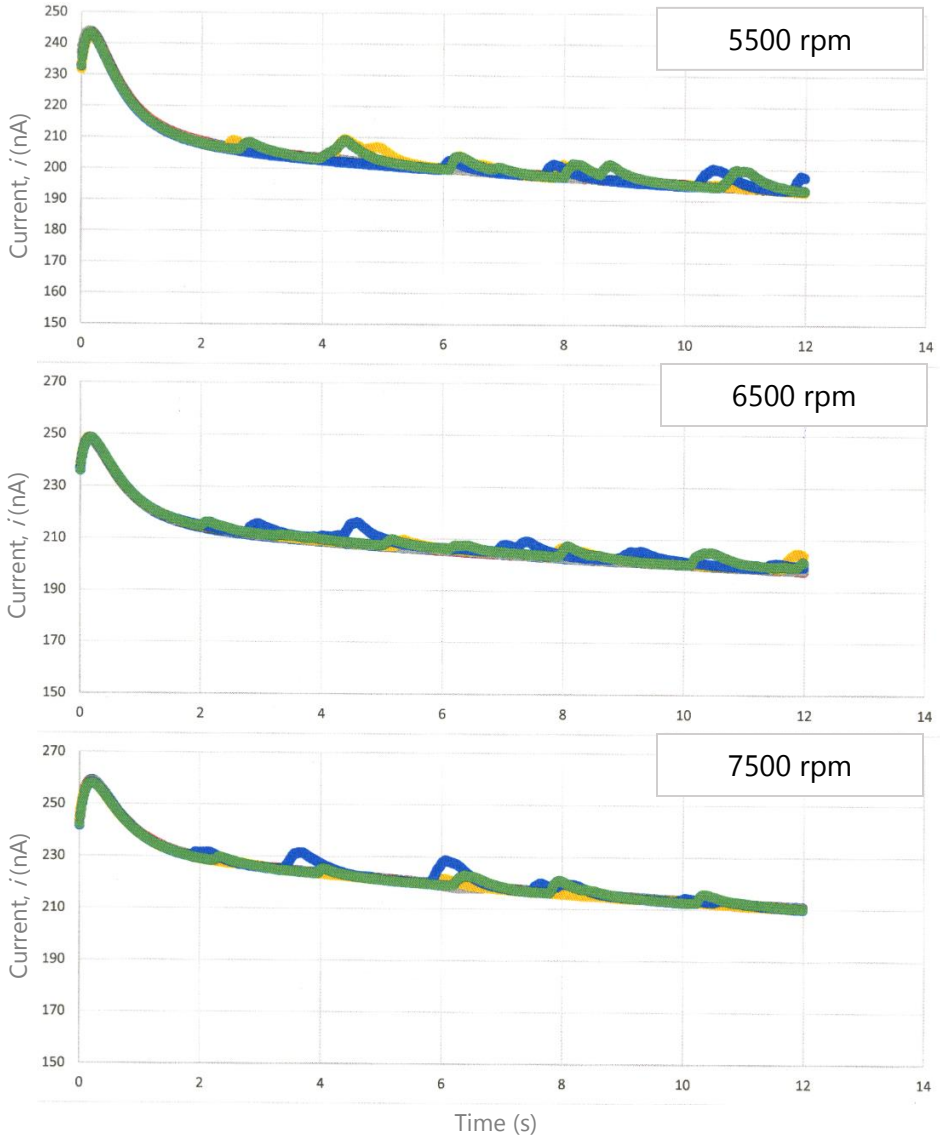

Figure 19 b. See above caption and 'wave tests' described in methods.

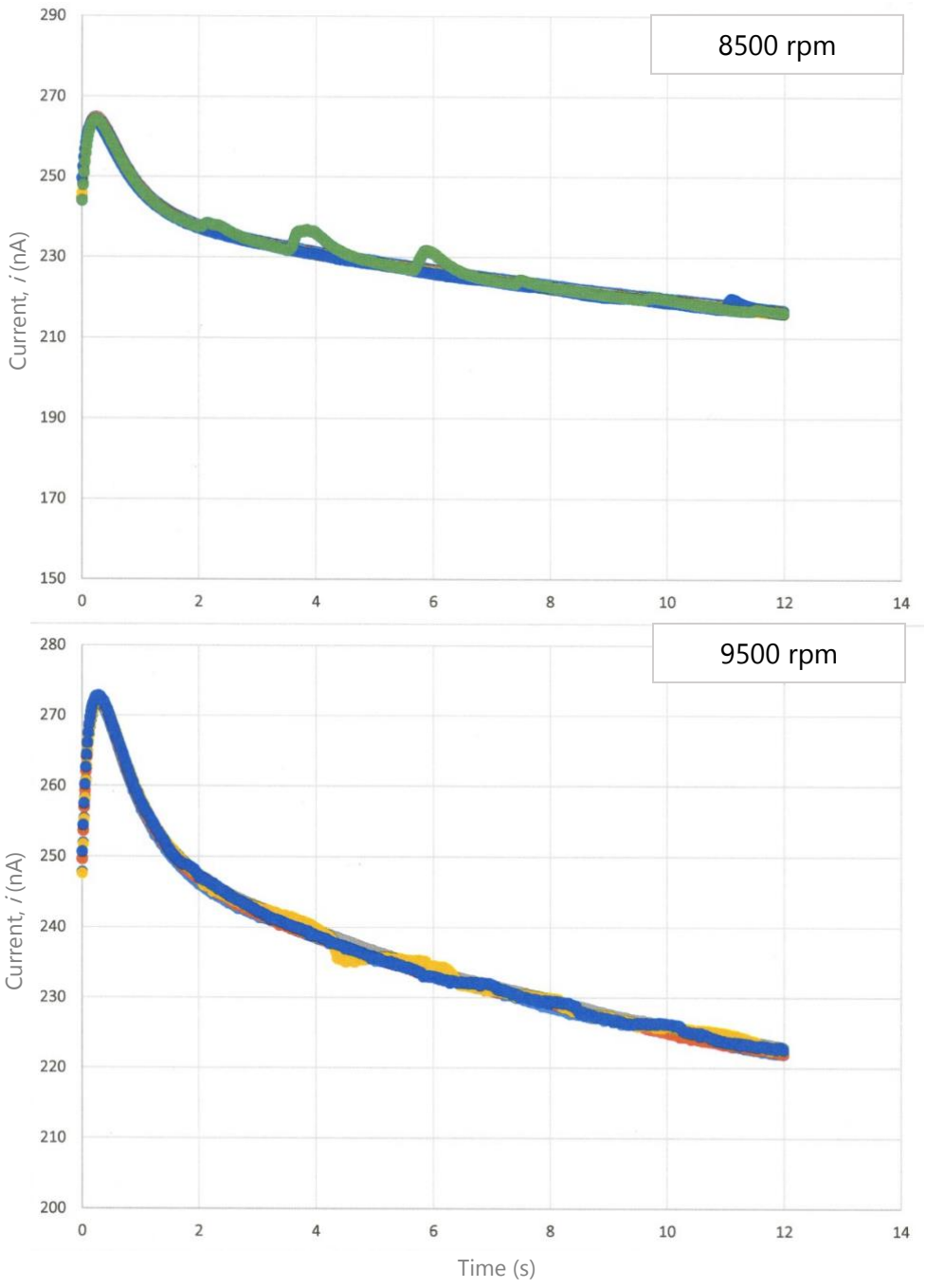

Figure 19 c. See above caption and 'wave tests' described in methods.

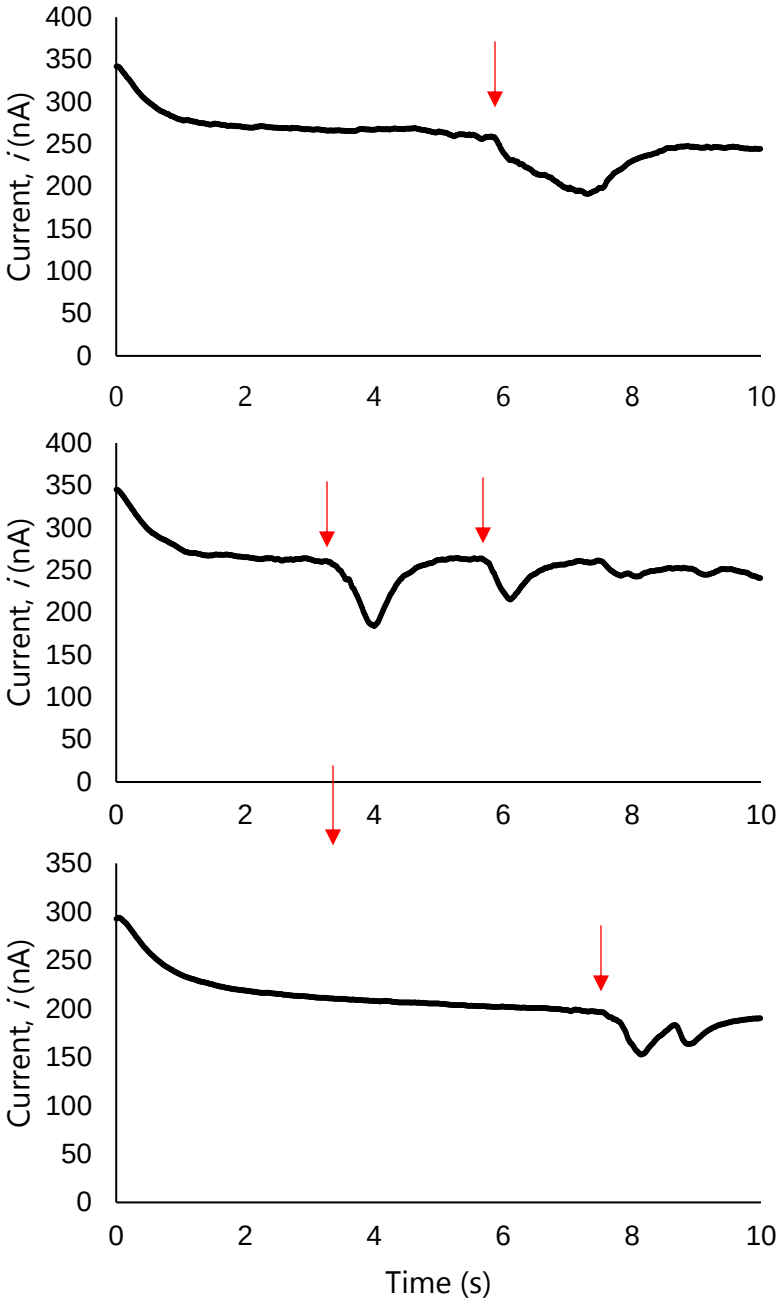

Figure 20. Examples of 'puff' response tests described in methods, performed in seawater at 1000 rpm. Red arrows indicate the point where the low-oxygen stream is first seen by the microdisc signal.

3.4 In situ measurements

Field deployments of the WER-I have been only partially successful thus far and require a second phase of development and testing. All deployments showed some quiescent periods where 12 s chronoamperometric curves appeared to exhibit steady-state conditions like those seen on the benchtop, implying a constant DO signal for that 12 s (Figure 21a) or a smoothing of any variations by the rotational-induced mixing. Conversely, various periods of non-steady signal were also observed (Figure 21b), but attempts to match these apparent DO concentration variations to a co-located microoptode record or to changes in velocities has not produced any results that are readily correlated. While some of these curves are only slightly non-steady, the more extreme examples (Figure 21c) have abrupt shifts (< 15 ms) similar to those seen in gated response time tests on the benchtop. However, more thoughtful examination reveals these shifts to be on the order of ~40 nA, which from calibrations is a very unrealistic >100 μM shift in DO. A possible interpretation of these jumps is intermittent stalling of the rotation speed. There are smooth rises and falls between these sharp drops that can be attributed to wave influence, but the massive decrease in signal can only be explained by sharp changes in DO transport to the electrode surface as could be caused by inconsistencies in the speed of rotation during the deployment.

It was also observed that signal values in the field started off much higher than pre-deployment calibrations, suggesting the superposition of an unusually large charging current. After ~60 min of measurement, signal returns tended to have decayed to match more closely with pre-deployment calibration values (Figure 22) but were not yet stable. The source of this capacitance effect is speculated to have been an artifact of placing the counter electrode (anode) too far away from the working cathode. It's also possible this effect stemmed from exposure to air or allowing too much time between conditioning in lab and deployment in the field.

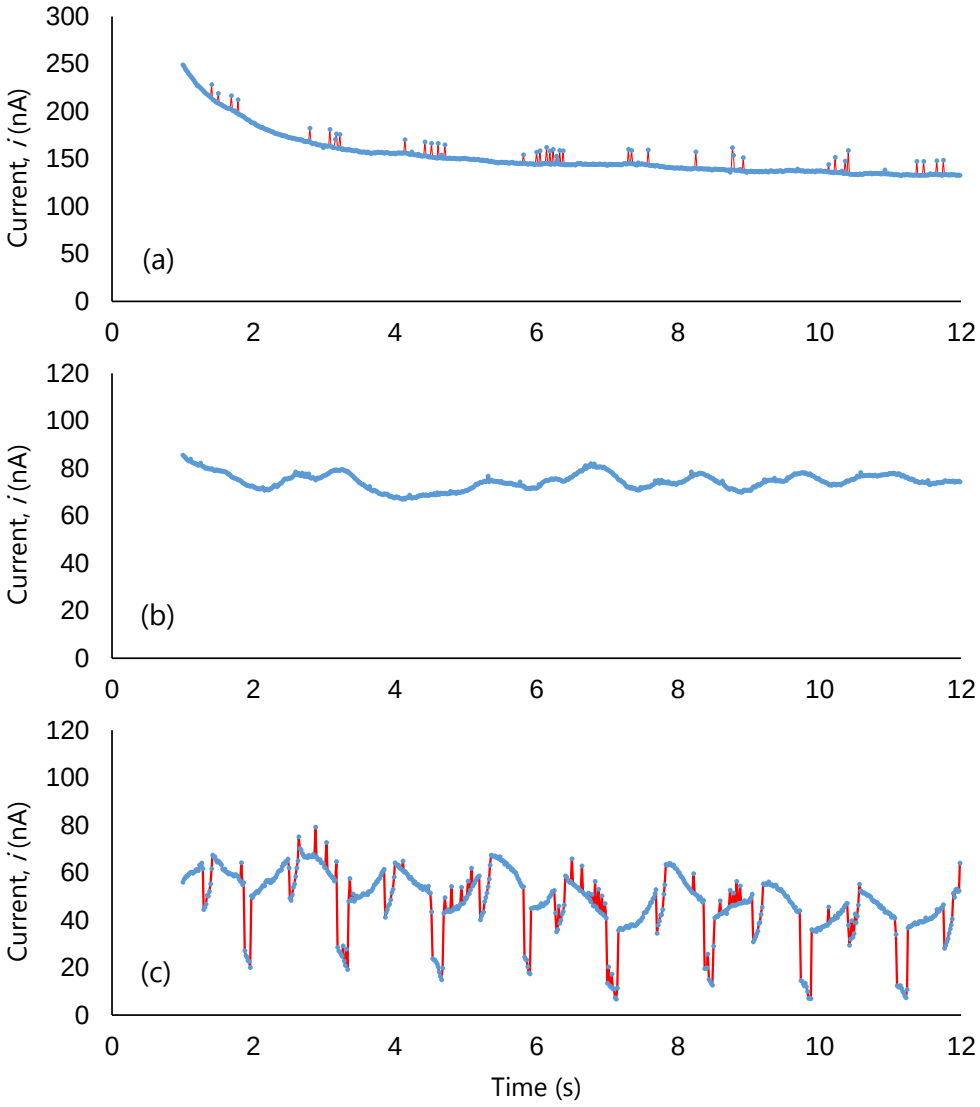

Figure 21. Examples of three different trends seen in chronoamperometric curves taken on Pt microdisc attached to the WER-I deployed in Yaquina Bay, Oregon. (a) is typical of a quiescent period, (b) indicative of mild non-steady flow conditions, and (c) showing an extreme case of signal fluctuations likely attributable to changes in rotation rate.

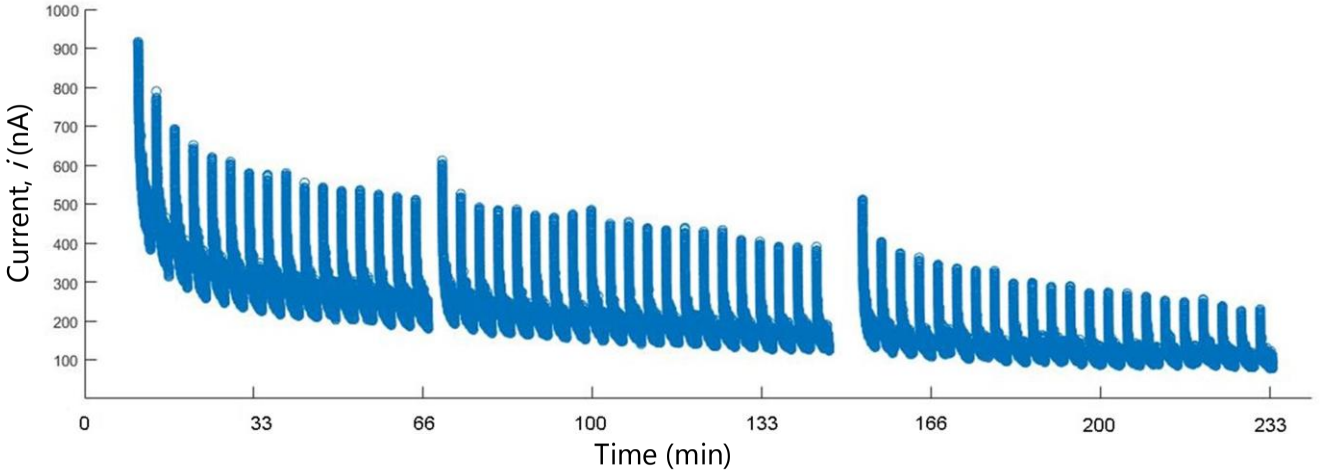

Figure 22. ~4 hours of in situ measurements on a Pt microdisc affixed to the WER-I. Plot includes the whole of each 12 s chronoamperometric curve, with the charging current not removed. This example from the third field deployment contains mostly smooth curves indicative of quiescent periods with minimal wave activity as was noted during this deployment. Evident are the high currents present initially that do not match pre-deployment calibrations, and the downward trend in current seen over the whole 4 hours that was analogous to the 50 – 100 scan conditioning period seen in benchtop measurements. Here, however, a period of steady state or near-calibration values were never truly reached.

4.0 Discussion

4.1 Signal behavior

Overall the electrode format detailed here showed a combination of linear responses to DO over a typical seawater range and high signal magnitudes. This contrasts with many capillary microsensors which, while linear in their responses, have much smaller output currents (picoamp ranges) that are recorded and translated to a concentration. The multiple order-of-magnitude increase in signal achieved with the induced flow of the rotational approach could help improve signal-to-noise ratios in certain applications. This higher signal from the increased flux has also been shown in benchtop seawater applications for other analytes to lower limits of detection by several orders of magnitude over equivalent stationary electrodes (Zirino 2002). This is likely true for oxygen, though no attempts to optimize for lower limits of detection were made in this work. The averaged signal output was also found to be consistent over many hours of operation (Figure 13), a finding that tracked very closely with previous studies on Pt microsensors applied to seawater (Atkinson et al. 1998, Pletcher and Sotiropoulos 1993, Sosna et al. 2008).

While a linear response to changes in oxygen concentration was resolved in the lab, this finding comes with many caveats. Calibrations were made by comparing

averages of the signal value for the final few seconds, or over particular 1 s intervals, within the chronoamperometric curve. Always the initial 3 seconds were ignored which, combined with the oxidative conditioning step, leaves only 67.5 – 78% of the total time taken up by each curve possibly resolvable as a brief time series measurement. Additionally, the most problematic caveat is that this curve is continually decaying, and in fact never reaches a truly asymptotic value as shown by experiments both with and without oxidative reconditioning (Figure 10).

In benchtop applications, chronoamperometric procedures aren't generally applied outside of steady state conditions as it complicates their interpretation, as has been encountered here. These typical benchtop applications are looking to the whole curve as an integrated representation of a single resolvable data point, not many points within the same curve as this investigation has attempted to do. Flume tests have shown that the electrode can clearly respond abruptly within the curve in confined laboratory conditions, and it was anticipated that in natural settings DO variation would appear as small fluctuations proportional to the actual in situ concentration shifts, all while the overall signal decays during the ~10 s period of measurement.

Furthermore, while a linear response was established, it must be noted that a significant number of sensor tests were unusable for a variety of reasons. Before reliable calibrations or measurements could be made, the electrode often had to be run in a continuous chronoamperometric mode for some time. This appeared to be a property of the electrode surface itself (perhaps dependent on polishing) and not a given matrix. It regularly took 50 – 100 chronoamperometric curves before a stable condition was reached and reliable calibrations could be developed. Conversely some experimental runs didn't require this period, and the sensor stabilized very quickly after just 5 – 10 curves. Electrical noise was also a major consideration and often made measurements unusable. Even when the system was contained in a Faraday cage there was some noise introduced through the rotator motor itself, both with the benchtop commercial model and WER-I.

Interestingly, the rotational dependence tests made here provide some information about the ORR itself, which is what the RDE approach has generally been used for in physicochemical studies. Were the reaction of interest (the ORR) to be limited in its overall rate at relevant time scales, the tight linear relation between current and $\omega^{1/2}$ would eventually reach a plateau where the current would be limited by the speed of the reaction, not the ability to force more reactant to its surface. With an upper limit on the commercial rotator used in the

lab of 9999 rpm, this plateau was not reached. While the ORR is a complex multi-electron reaction that cannot benefit from tools like Kotecky-Levich plots (Bard and Faulkner 1980), this investigation was only attempting to measure any first-order influences at the given timescales of interest (milliseconds) not to investigate the reaction itself as has been done exhaustively by whole communities of researchers. The use of a larger Pt RDE in early assessments gave confidence that there would be little influence of site heterogeneity on the overall output of a much smaller sensor. Were this to be the case, an inconsistent $\omega^{1/2}$ vs i comparison would have been seen (Figure 16). Good agreement was also seen between rotation rate and signal output on the microdisc when placed in a slow background flow field (Figure 17), though it must be noted this was done at very low flows (~2 cm/s) compared to those present in many natural settings, including those encountered in field deployments described in this study. Future work requires a repeat of this assessment in a much larger flume with the truly in situ WER where flow can be tightly controlled and turbulent structure of varying properties introduced to the sensor in a controlled manner.

4.2 Response characteristics

The most compelling findings of this work were the reproducible rapid responses to large abrupt shifts (50 – 100 μM changes) in DO. This t_{90}% = 50 ms average is roughly an order of magnitude faster than any reported DO sensor and speaks to the possible benefits of hydrodynamic sensors in future development avenues. It's also suspected that the ~20 ms lower limit that appeared to be reached was a limitation of the response apparatus used (along with the large size of the rotating head). It is speculated that the response could actually be pushed much lower, possibly only limited by the speed of the ORR itself. Because the response time tests in this study involved a fairly crude operation (moving the sensor down a track by hand) any attempts to make fine comparisons of the response time's dependence on either rotation rate or temperature of the solution were not attempted. It would seem likely that there is a mechanistic dependence of the response time on the rate of rotation as that will largely dictate the boundary layer thickness at the electrode surface. This is similarly true for the considerations of temperature's influence on diffusion for its role in eq. 4 generally and the diffusion coefficient for oxygen in this case specifically. A consistent mechanically driven response apparatus is all that would be needed to evaluate these dependencies.

4.3 Mixing and stirring artifacts

With a thin boundary layer and 'self-flushing' mechanism, the RDE sensor is able to respond quickly to rapid shifts in DO. Though it's evident from the response tests that the size of electrode head used in this study, not the sensing surface itself, introduces mixing artifacts to the signal, such that water parcels of small size but varying DO are subject to a kind of in situ integration by mixing before solution reaches near the electrode surface. A head size and geometry of significantly smaller proportions would afford less of these mixing artifacts and likely give a cleaner signal while still benefiting from a very thin boundary layer. Use of a membrane coating would likely reduce the magnitude of this flow-induced signal bias but not eliminate it, as the same stirring artifacts are documented for stationary microelectrodes with membranes in other applications (Gust et al. 1987, Reimers et al. 2016).

These external-to-the-electrode mixing effects were also seen in the "puff" tests conducted. During these tests there was never a clean break between one solution to another as in the gated response tests. Instead what was seen appeared to be a smooth drop and rise back to normal levels (Figure 21) that can be speculated as likely a mixing of the anoxic water passing by the rotating head with the oxic background flow. The rotation of the head was likely spinning the parcel of anoxic solution away from the sensor as much as it was pulling it

towards the sensor surface, mixing the whole solution rather than sensing a sharp change as a discrete parcel moved toward it. With both the commercial and submersible rotators, seeing small scale (<3 cm) water parcels in their intact form was impossible as any non-dispersing parcel was obliterated by the rotational-induced mixing as it approached the head. While assessments of the influence of this rotational-flow were not made specifically, the highest rates of rotation, had influences several centimeters away from the sensor (Levich 1962). It is likely that the diameter of electrode head combined with the rate of rotation dictate an effective "mixing distance" that the electrode is drawing fluid from.

The most discouraging finding of this work was decidedly the flow-induced biasing of the electrode signal under wave motions (Figure 19)). Small flume tests showed serious artifacts introduced to the signal by wave motion, and while running the electrode at higher rates of rotation reduced this wave influence, faster rates were not a perfect solution. For one, the rates that actually began to see the "wash out" of the wave signal were very high (>5000 rpm). While certainly it's possible to construct in situ rotators to run at these high rates, the tests in the flume show that these high rates introduce an unsettling amount of rotational-induced mixing. While tests were performed in confined flumes where momentum communication with the boundaries of the flume likely helped to make the mixing worse, it was so pronounced an issue that the only conclusion is

the current size of rotator head and shaft is not viable for “fine point” measurements under variable flow.

4.4 Field considerations

As mentioned, all field measurements to date have been unsuccessful in measuring in situ DO concentrations in a prolonged time series mode with the WER-I and a Pt microdisc.

With the rotational format there are some added mechanical issues in situ that weren’t appreciated until in situ deployments were made. Increased mass flux, the thing that theoretically benefits the system’s response time also comes with a drawback, that it is forcing everything suspended in solution at the electrode surface. In filtered media this isn’t a problem, but natural waters contain a wide combination of colloidal and solid phase particles of varying sizes. It was seen during post-deployment microscope examinations that the Pt surface was being blasted by these fine particles, with visible gouges and scrapes in both the Pt surface and the surrounding plastic. These marks would affect the sensor response two-fold: first by exposing fresh electrode surface that will immediately be more reactive than the conditioned surface that had been in its place, and by increasing the overall surface area of the electrode. This last effect is particularly problematic both because of the already small electrode size and the

dependence of signal output on surface area predicted by the equations defining electrode output (Eq 1, 2, 4).

4.5 Prototype performance

Finally, a WER-I was built as a first-order proof of concept and has shown that a functional submersible rotator is possible and not difficult to construct. The limitations of this prototype include its lack of electrical shielding, size, depth rating, rotation rate and control, electrode signal path internally, and lack of integrated anode.

Overall the housing for the WER-I is much larger than it needs to be and future iterations will certainly reduce this size. The shaft itself is also quite long and large in diameter. As detailed, the size of the shaft and tip diameter is a main factor driving the rotational-induced mixing and a smaller shaft diameter would reduce this. The 15 mm of diameter currently employed was chosen to reduce wobble over time that would damage bulkhead seals. The most important geometric consideration is surely the electrode head itself. It is very likely that a different head design informed by fluid dynamics work either in aerospace or maritime engineering could provide smoother transport of analyte that further reduces rotational-induced flow to the external system. Studies varying the size of the non-reactive portion of the disc tip would be useful, and may find a better

optimization between reducing mixing of the surroundings and maintaining the benefits of a thin boundary layer.

The rate of rotation and its steady maintenance were also a recurring issue with this prototype. Features of commercial rotators are that they carry a relatively noise-free signal from a spinning shaft to an instrument, and they maintain a very consistent rate of rotation. This was less true for the prototype here which had an upper limit of rotation ~1500 rpm, which is both quite low compared to the 10,000 rpm limit of benchtop models, and well below any vague “wash-out” range discernable from the wave tests performed in the lab (the range speculated here is somewhere between 2000 – 4000 rpm). This is likely a main culprit in the stirring effects seen throughout the described deployments. Additionally, this prototype system also had serious issues in maintaining a consistent rate of rotation. This was both an issue out of water during calibrations where the shaft would stall from lack of lubricating material (external solution), as well as in situ where the shaft would regularly fluctuate between the 1000 and 100 rpm ranges over the span of seconds.

Lastly, there were electronics issues. Noise generated by the rotating motor impacted the RDE signal. The internal working electrode signal path would have benefitted from shielding to prevent the introduction of motor noise to the

relatively small signal of the sensor. While using a hardware filter built into the DLK potentiostat helped to remove noise, this is not ideal, as it prevents a clean separation of any remaining noise influence and possibly real signal. This is an easily remedied problem that is first to be changed in subsequent iterations.

Another benefit would be the integration of an anode into the rotating head itself, possibly as a ring electrode around the primary working electrode (Hsueh et al. 1983). Bringing the anode and cathode closer together will reduce both the time of initial charge drop and likely return cleaner more consistent readings (Sosna et al. 2007). Uncertainties from variability in the speed and direction of flow that could influence how the anode and cathode communicate with each other would also be reduced or eliminated in this configuration.

5.0 Comments and Recommendations

While the results of this study indicate that rotational electrodes, or some other hydrodynamic sensor format, have some key benefits, there is much to be done to translate these sensors to in situ use. Resolving high frequency DO signals remains a significant challenge for sensors of all types.

With no other chemical sensors able to respond at comparable rates, the accuracy of any measurement frequency $> 2\ \mathrm{Hz}$ will be difficult to truly verify. Future tests in settings with mixing of disparate water masses varied in both oxygen and temperature may hold the key, as thermistors are one of the only sensors capable of responding at rates faster than those trying to be resolved with this RDE approach. In this scenario co-located temperature and RDE measurements could bealigned, provided that temperature is mixed conservatively with respect to O_2 in the given setting.

This too, however, requires a further developed rotating system, one which utilizes a much smaller shaft and head geometry to reduce its own influence on the surrounding system while possibly still capturing natural flow structures without obliterating them. This speaks to careful and controlled flume studies with laser Doppler velocimeters able to resolve 3-dimensional flow field patterns at and around the sensor head in flumes of adequately large size to eliminate any

boundary influences. It is possible that vibrational microelectrodes, now regularly developed for environmental measurements, could produce similar boundary layer benefits without the drawback of rotational-induced flow.

While much of the hydrodynamic theory of RDEs has been settled by Levich and his contemporaries decades ago, they rarely considered the constraints of a fluid system without boundaries and regularly not at steady state as is seen in the ocean and other natural bodies. As a result this may complicate what we're able to discern or model is happening during the complex interactions of a rotated shaft exposed to both advective and turbulent motions of the varied length and time scales present in moving fluids. Ultimately it may be found these non-steady influences introduce too much uncertainty regardless of the electrode material or analyte of interest. Outside of free-fall profiling scenarios where the sensor wouldn't be as affected by non-steady flow, it's likely that any fixed-point RDE application, even if analytically constrainable, will require secondary measurement of fluid motion at or near its electroactive surface.

The future of an in situ rotational approach is far from certain, though O_2 reduction on Pt is only one of countless materials and procedures that could be examined and applied in situ. Likely any future for this format of approach lies not in fast response applications, but in low concentrations. As noted many times

the RDE format has been shown time and again to lower limits of detection for many analytes in seawater. Most of the issues that have been detailed with the current system come from the attempt to develop a sensor for eddy covariance applications. Systems optimized and specific to trace metal detection at sub-nanomolar levels have already been applied in flow-lines to estuaries and shipboard. Similarly non-rotating solid state electrodes have been used regularly in the water column for decades with matrix influences well described. The leap to put these proven approaches on a spinning shaft is a short one if you already have a functioning submersible rotator and reliable electrochemical procedure.

This investigation has shown that there are some intriguing benefits to the implementation of sensors with deliberate control of hydrodynamics at their interface. The attempt to fit a well-understood chronoamperometric approach to determine dissolved oxygen on an unshielded platinum microdisc may not have been the best fit, but it has allowed the measurement of response rates an order of magnitude shorter than reported for any in situ oxygen sensor. Alternative constructions, electrode materials and procedures may in the future lead to systems with reliably stable readings able to be applied for DO in fixed-point Eulerian or fast water column profiling applications that can benefit from this rapid response induced by rotation.

6.0 References

Atkinson, M. J., Thomas, F. I. M., Larson, N., Terrill, E., Morita, K., & Liu, C. C. (1995). A micro-hole potentiostatic oxygen sensor for oceanic CTDs. *Deep Sea Research Part I: Oceanographic Research Papers*, *42*(5), 761-771.

Atkinson, M. J., Thomas, F. I. M., & Larson, N. (1996). Effects of pressure on oxygen sensors. *Journal of Atmospheric and Oceanic Technology*, *13*(6), 1267-1274.

Banks, C. E., Simm, A. O., Bowler, R., Dawes, K., & Compton, R. G. (2005). Hydrodynamic electrochemistry: design for a high-speed rotating disk electrode. *Analytical chemistry*, *77*(6), 1928-1930.

Bennett, C. W., Kenny, H. C., & Dugliss, R. P. (1914). Electrodeposition of nickel. *The Journal of Physical Chemistry*, *18*(5), 373-384.

Berg, P., Røy, H., Janssen, F., Meyer, V., Jørgensen, B. B., Huettel, M., & de Beer, D. (2003). Oxygen uptake by aquatic sediments measured with a novel non-invasive eddy-correlation technique. *Marine Ecology Progress Series*, *261*, 75-83.

Berg, P., Glud, R. N., Hume, A., Stahl, H., Oguri, K., Meyer, V., & Kitazato, H. (2009). Eddy correlation measurements of oxygen uptake in deep ocean sediments. *Limnology and Oceanography: Methods*, *7*(8), 576-584.

Berg, P., Koopmans, D. J., Huettel, M., Li, H., Mori, K., & Wüest, A. (2016). A new robust oxygen-temperature sensor for aquatic eddy covariance measurements. *Limnology and Oceanography: Methods*, *14*(3), 151-167.

Bittig, H. C., & Körtzinger, A. (2015). Tackling oxygen optode drift: Near-surface and in-air oxygen optode measurements on a float provide an accurate in situ reference. *Journal of Atmospheric and Oceanic Technology*, *32*(8), 1536-1543.

Bittig, H. C., & Körtzinger, A. (2017). Update on response times, in-air measurements, and in situ drift for oxygen optodes on profiling platforms. *Ocean Science*, *13*(1), 1-11.

Broecker, W. S., & Peng, T. H. (1974). Gas exchange rates between air and sea. *Tellus*, *26*(1-2), 21-35.

Bruland, K. W., Coale, K. H., & Mart, L. (1985). Analysis of seawater for dissolved cadmium, copper and lead: An intercomparison of voltammetric and atomic absorption methods. *Marine Chemistry*, *17*(4), 285-300.

Bushinsky, S. M., & Emerson, S. (2015). Marine biological production from in situ oxygen measurements on a profiling float in the subarctic Pacific Ocean. *Global Biogeochemical Cycles*, *29*(12), 2050-2060.

Bushinsky, S. M., Emerson, S. R., Riser, S. C., & Swift, D. D. (2016). Accurate oxygen measurements on modified Argo floats using in situ air calibrations. *Limnology and Oceanography: Methods*, *14*(8), 491-505.

Carritt, D. E., & Kanwisher, J. W. (1959). Electrode system for measuring dissolved oxygen. *Analytical Chemistry*, *31*(1), 5-9.

Chipman, L., Huettel, M., Berg, P., Meyer, V., Klimant, I., Glud, R., & Wenzhoefer, F. (2012). Oxygen optodes as fast sensors for eddy correlation measurements in aquatic systems. *Limnology and Oceanography: Methods*, *10*(5), 304-316.

Clark Jr, LC; Wolf, R; Granger, D; Taylor, Z (1953). "Continuous recording of blood oxygen tensions by polarography". *Journal of Applied Physiology*. **6** (3): 189–93.

Crimmins, D., Deacutis, C., Hinchey, E., Chintala, M., Cicchetti, G., & Blidberg, D. (2005, June). Use of a long endurance solar powered autonomous underwater vehicle (SAUV II) to measure dissolved oxygen concentrations in Greenwich Bay, Rhode Island, USA. In *Europe Oceans 2005* (Vol. 2, pp. 896-901). IEEE.

Curtin, T. B., Crimmins, D. M., Curcio, J., Benjamin, M., & Roper, C. (2005). Autonomous underwater vehicles: trends and transformations. *Marine Technology Society Journal*, *39*(3), 65-75.

Daly, K. L., Byrne, R. H., Dickson, A. G., Gallager, S. M., Perry, M. J., & Tivey, M. K. (2004). Chemical and biological sensors for time-series research: Current status and new directions. *Marine Technology Society Journal*, *38*(2), 121-143.

D'Asaro, Eric A., and Craig McNeil. (2013) "Calibration and stability of oxygen sensors on autonomous floats." *Journal of Atmospheric and Oceanic Technology* 30.8: 1896-1906.

Delauney, L., Compere, C., & Lehaitre, M. (2010). Biofouling protection for marine environmental sensors. *Ocean Science*, *6*(2), 503-511.

Denuault, G. (2009). Electrochemical techniques and sensors for ocean research. *Ocean Science*, *5*(4), 697-710.

Donis, D., Holtappels, M., Noss, C., Cathalot, C., Hancke, K., Polsenaere, P., ... & McGinnis, D. F. (2015). An assessment of the precision and confidence of aquatic eddy correlation measurements. *Journal of Atmospheric and Oceanic Technology*, *32*(3), 642-655.

Falter, J. L., Lowe, R. J., Atkinson, M. J., Monismith, S. G., & Schar, D. W. (2008). Continuous measurements of net production over a shallow reef community using a modified Eulerian approach. *Journal of Geophysical Research: Oceans*, *113*(C7).

Frary, F. C. (1907). Rapid analysis by electrolysis without rotating electrodes. *Journal of the American Chemical Society*, *29*(11), 1592-1596.

Garcia, H. E., & Gordon, L. I. (1992). Oxygen solubility in seawater: Better fitting equations. *Limnology and oceanography*, *37*(6), 1307-1312.

Gieseke, A., & de Beer, D. (2008). Section 8 update: Use of microelectrodes to measure in situ microbial activities in biofilms, sediments, and microbial

mats. In *Molecular Microbial Ecology Manual* (pp. 3483-3514). Springer Netherlands.

Gouin, J. F., Baros, F., Birot, D., & Andre, J. C. (1997). A fibre-optic oxygen sensor for oceanography. *Sensors and Actuators B: Chemical*, *39*(1-3), 401-406.

Gundersen, J. K., Ramsing, N. B., & Glud, R. N. (1998). Predicting the signal of O_2 microsensors from physical dimensions, temperature, salinity, and O_2 concentration. *Limnology and Oceanography*, *43*(8), 1932-1937.

Gust, G., Booij, K., Helder, W., & Sundby, B. (1987). On the velocity sensitivity (stirring effect) of polarographic oxygen microelectrodes. *Netherlands Journal of Sea Research*, *21*(4), 255-263.

Himmelblau, D. M. (1964). Diffusion of dissolved gases in liquids. *Chemical Reviews*, *64*(5), 527-550.

Hintermann, H. E., & Suter, E. (1965). High-speed rotating disk electrode unit. *Review of Scientific Instruments*, *36*(11), 1610-1614.

Holtappels, M., Glud, R. N., Donis, D., Liu, B., Hume, A., Wenzhöfer, F., & Kuypers, M. M. (2013). Effects of transient bottom water currents and oxygen concentrations on benthic exchange rates as assessed by eddy correlation measurements. *Journal of Geophysical Research: Oceans*, *118*(3), 1157-1169.

Holtappels, M., Noss, C., Hancke, K., Cathalot, C., McGinnis, D. F., Lorke, A., & Glud, R. N. (2015). Aquatic eddy correlation: Quantifying the artificial flux caused by stirring-sensitive O_2 sensors. *PLoS One*, *10*(1), e0116564.

Holst, G., Glud, R. N., Kühl, M., & Klimant, I. (1997). A microoptode array for fine-scale measurement of oxygen distribution. *Sensors and Actuators B: Chemical*, *38*(1-3), 122-129.

Hsueh, K. L., Gonzalez, E. R., & Srinivasan, S. (1983). Electrolyte effects on oxygen reduction kinetics at platinum: a rotating ring-disc electrode analysis. *Electrochimica Acta*, *28*(5), 691-697.

Hutton, L., Newton, M. E., Unwin, P. R., & Macpherson, J. V. (2008). Amperometric oxygen sensor based on a platinum nanoparticle-modified polycrystalline boron doped diamond disk electrode. *Analytical chemistry*, *81*(3), 1023-1032.

Johnson, K. S., Barry, J. P., Coletti, L. J., Fitzwater, S. E., Jannasch, H. W., & Lovera, C. F. (2011). Nitrate and oxygen flux across the sediment-water interface observed by eddy correlation measurements on the open continental shelf. *Limnology and Oceanography: Methods*, *9*(11), 543-553.

Johnson, K. S., Plant, J. N., Riser, S. C., & Gilbert, D. (2015). Air oxygen calibration of oxygen optodes on a profiling float array. *Journal of Atmospheric and Oceanic Technology*, *32*(11), 2160-2172.

Katsounaros, I., Schneider, W. B., Meier, J. C., Benedikt, U., Biedermann, P. U., Cuesta, A., ... & Mayrhofer, K. J. (2013). The impact of spectator species on the interaction of H_2O_2 with platinum–implications for the oxygen reduction reaction pathways. *Physical Chemistry Chemical Physics*, *15*(21), 8058-8068.

Kanwisher, John (1959). Polarographic Oxygen Electrode. *Limnology and Oceanography*. **4** (2): 210–217

Körtzinger, A., Schimanski, J., & Send, U. (2005). High quality oxygen measurements from profiling floats: A promising new technique. *Journal of Atmospheric and Oceanic Technology*, *22*(3), 302-308.

Lee, J. H., Lim, T. S., Seo, Y., Bishop, P. L., & Papautsky, I. (2007). Needle-type dissolved oxygen microelectrode array sensors for in situ measurements. *Sensors and Actuators B: Chemical*, *128*(1), 179-185.

Levich, V. G. (1962). Physicochemical hydrodynamics. Prentice-Hall. Princeton, NJ.

Lindstrom, E., Gunn, J., Fischer, A., McCurdy, A., Glover, L. K., Alverson, K., ... & Clark, C. (2012). A framework for ocean observing. *Proceedings of the Ocean Information for Society: Sustaining the Benefits, Realizing the Potential, Venice, Italy*, *2125*.

Lorrai, C., McGinnis, D. F., Berg, P., Brand, A., & Wüest, A. (2010). Application of oxygen eddy correlation in aquatic systems. *Journal of Atmospheric and Oceanic Technology*, *27*(9), 1533-1546.

Luther III, G. W., Rozan, T. F., Taillefert, M., Nuzzio, D. B., Di Meo, C., Shank, T. M., ... & Cary, S. C. (2001). Chemical speciation drives hydrothermal vent ecology. *Nature*, *410*(6830), 813.

Ma, S., Luther III, G. W., Keller, J., Madison, A. S., Metzger, E., Emerson, D., & Megonigal, J. P. (2008). Solid-state Au/Hg microelectrode for the investigation of Fe and Mn cycling in a freshwater wetland: Implications for methane production. *Electroanalysis: An International Journal Devoted to Fundamental and Practical Aspects of Electroanalysis*, *20*(3), 233-239.

McGinnis, D. F., Sommer, S., Lorke, A., Glud, R. N., & Linke, P. (2014). Quantifying tidally driven benthic oxygen exchange across permeable sediments: An aquatic eddy correlation study. *Journal of Geophysical Research: Oceans*, *119*(10), 6918-6932.

Merikhi, A., Berg, P., Meyer, V., & Huettel, M. (2018). Jet-nozzle method for measuring response times of scalar sensors used in liquids and gases. *Limnology and Oceanography: Methods*, *16*(8), 475-483.

Mikkelsen, Ø., van den Berg, C. M., & Schrøder, K. H. (2006). Determination of labile iron at low nmol l− 1 levels in estuarine and coastal waters by anodic stripping voltammetry. *Electroanalysis: An International Journal Devoted to Fundamental and Practical Aspects of Electroanalysis*, *18*(1), 35-43.

Moore, T. S., Nuzzio, D. B., Deering, T. W., Taillefert, M., & Luther III, G. W. (2007). Use of voltammetry to monitor O_2 using Au/Hg electrodes and to control physical sensors on an unattended observatory in the Delaware Bay. *Electroanalysis: An International Journal Devoted to Fundamental and Practical Aspects of Electroanalysis*, *19*(19-20), 2110-2116.

Mullaugh, K. M., Luther III, G. W., Ma, S., Moore, T. S., Yücel, M., Becker, E. L., ... & Pierson, B. K. (2008). Voltammetric (Micro) Electrodes for the In Situ Study of

Fe^{2+} Oxidation Kinetics in Hot Springs and $S_2O_3^{2-}$ Production at Hydrothermal Vents. *Electroanalysis: An International Journal Devoted to Fundamental and Practical Aspects of Electroanalysis*, *20*(3), 280-290.

Nei, L., & Compton, R. G. (1996). An improved Clark-type galvanic sensor for dissolved oxygen. *Sensors and Actuators B: Chemical*, *30*(2), 83-87.

Oldham, C. (1994). A fast-response oxygen sensor for use on fine-scale and microstructure CTD profilers. *Limnology and oceanography*, *39*(8), 1959-1966.

Pletcher, D., & Sotiropoulos, S. (1993). A study of cathodic oxygen reduction at platinum using microelectrodes. *Journal of Electroanalytical Chemistry*, *356*(1-2), 109-119.

Pletcher, D., & Sotiropoulos, S. (1996). Towards a microelectrode sensor for the determination of oxygen in waters. *Analytica chimica acta*, *322*(1-2), 83-90.

Santegoeds, C. M., Schramm, A., & De Beer, D. (1998). Microsensors as a tool to determine chemical microgradients and bacterial activity in wastewater biofilms and flocs. *Biodegradation*, *9*(3-4), 159-167.

Shinozaki, K., Zack, J. W., Richards, R. M., Pivovar, B. S., & Kocha, S. S. (2015). Oxygen reduction reaction measurements on platinum electrocatalysts utilizing rotating disk electrode technique I. Impact of impurities, measurement protocols and applied corrections. *Journal of The Electrochemical Society*, *162*(10), F1144-F1158.

Sosna, M., Denuault, G., Pascal, R. W., Prien, R. D., & Mowlem, M. (2008). Field assessment of a new membrane-free microelectrode dissolved oxygen sensor for water column profiling. *Limnology and Oceanography: Methods*, *6*(4), 180-189.

Suzuki, H., Hirakawa, T., Watanabe, I., & Kikuchi, Y. (2001). Determination of blood pO2 using a micromachined Clark-type oxygen electrode. *Analytica Chimica Acta*, *431*(2), 249-259.

Reimers, C. E., Özkan-Haller, H. T., Albright, A. T., & Berg, P. (2016). Microelectrode velocity effects and aquatic eddy covariance measurements under waves. *Journal of Atmospheric and Oceanic Technology*, *33*(2), 263-282.

Revsbech, N. P., & Ward, D. M. (1983). Oxygen microelectrode that is insensitive to medium chemical composition: use in an acid microbial mat dominated by Cyanidium caldarium. *Applied and Environmental Microbiology*, *45*(3), 755-759.

Revsbech, N. P. (1989). An oxygen microsensor with a guard cathode. *Limnology and Oceanography*, *34*(2), 474-478.

Riso, R. D., Le Corre, P., & Chaumery, C. J. (1997). Rapid and simultaneous analysis of trace metals (Cu, Pb and Cd) in seawater by potentiometric stripping analysis. *Analytica Chimica Acta*, *351*(1-3), 83-89.

Rozan, T. F., Theberge, S. M., & Luther III, G. (2000). Quantifying elemental sulfur (S^0), bisulfide (HS^-) and polysulfides (S_x^{2-}) using a voltammetric method. *Analytica Chimica Acta*, *415*(1-2), 175-184.

Takeshita, Y., Martz, T. R., Johnson, K. S., Plant, J. N., Gilbert, D., Riser, S. C., ... & Tilbrook, B. (2013). A climatology-based quality control procedure for profiling float oxygen data. *Journal of Geophysical Research: Oceans*, *118*(10), 5640-5650.

Taillefert, M., Luther III, G. W., & Nuzzio, D. B. (2000). The application of electrochemical tools for in situ measurements in aquatic systems. *Electroanalysis: An International Journal Devoted to Fundamental and Practical Aspects of Electroanalysis*, *12*(6), 401-412.

Tengberg, A., Hovdenes, J., Andersson, H. J., Brocandel, O., Diaz, R., Hebert, D., ... & Rey, F. (2006). Evaluation of a lifetime-based optode to measure oxygen in aquatic systems. *Limnology and Oceanography: Methods*, *4*(2), 7-17.

Wakabayashi, N., Takeichi, M., Itagaki, M., Uchida, H., & Watanabe, M. (2005). Temperature-dependence of oxygen reduction activity at a platinum electrode in an acidic electrolyte solution investigated with a channel flow double electrode. *Journal of Electroanalytical Chemistry*, *574*(2), 339-346.

Wang, B. (2005). Recent development of non-platinum catalysts for oxygen reduction reaction. *Journal of Power Sources*, *152*, 1-15.

Winkler, L. W. 1888. The determination of dissolved oxygen in water. Berichte der Deutschen Chemischen Gesellschaft 21:2843-2854

Zirino, A., De Marco, R., Rivera, I., & Pejcic, B. (2002). The influence of diffusion fluxes on the detection limit of the jalpaite copper Ion-selective electrode. *Electroanalysis: An International Journal Devoted to Fundamental and Practical Aspects of Electroanalysis*, *14*(7-8), 493-498.